

**EFFECTS OF Zn AND Al ON CORROSION  
CHARACTERISTICS OF Sn-1.0Ag-0.5Cu ALLOYS**

**NURUL LIYANA BINTI KAMARUZAMAN**

**FACULTY OF ENGINEERING  
UNIVERSITY OF MALAYA  
KUALA LUMPUR**

**2018**

EFFECTS OF Zn AND Al ON CORROSION  
CHARACTERISTICS OF Sn-1.0Ag-0.5Cu ALLOYS

NURUL LIYANA BINTI KAMARUZAMAN

DISSERTATION SUBMITTED IN FULFILMENT OF THE  
REQUIREMENTS FOR THE DEGREE OF MASTER OF  
ENGINEERING SCIENCE

FACULTY OF ENGINEERING  
UNIVERSITY OF MALAYA  
KUALA LUMPUR

2018

**UNIVERSITY OF MALAYA**  
**ORIGINAL LITERARY WORK DECLARATION**

Name of Candidate: **Nurul Liyana Bt. Kamaruzaman**

Matric No: **KGA 130087**

Name of Degree: **Master of Engineering Science**

Title of Project Paper/Research Report/Dissertation/Thesis ("this Work"):

**Effects of Zn and Al on corrosion characteristics of Sn-1.0Ag-0.5Cu alloys**

Field of Study: Master of Engineering Science

I do solemnly and sincerely declare that:

- (1) I am the sole author/writer of this Work;
- (2) This Work is original;
- (3) Any use of any work in which copyright exists was done by way of fair dealing and for permitted purposes and any excerpt or extract from, or reference to or reproduction of any copyright work has been disclosed expressly and sufficiently and the title of the Work and its authorship have been acknowledged in this Work;
- (4) I do not have any actual knowledge nor do I ought reasonably to know that the making of this work constitutes an infringement of any copyright work;
- (5) I hereby assign all and every rights in the copyright to this Work to the University of Malaya ("UM"), who henceforth shall be owner of the copyright in this Work and that any reproduction or use in any form or by any means whatsoever is prohibited without the written consent of UM having been first had and obtained.
- (6) I am fully aware that if in the course of making this Work I have infringed any copyright whether intentionally or otherwise, I may be subject to legal action or any other action as may be determined by UM.

Candidate's Signature

Date

Subscribed and solemnly declared before,

Witness's Signature

Date

Name:

Designation

# EFFECTS OF Zn AND Al ON CORROSION CHARACTERISTICS OF Sn-1.0Ag-0.5Cu ALLOYS

## ABSTRACT

In the past few years, tin-lead (Sn-Pb) solder alloys had been popularly used in the electronic industries especially in packaging. However, lead and lead containing alloys have been banned because of environmental and health concerns. Recently, efforts are being made to develop a usable lead-free solder to substitute tin-lead based solder alloys. Comparing to other solders, tin-silver-copper (Sn-Ag-Cu) free solder alloys seem to be the best alternative to replace traditional lead-tin based solder alloys. In the present study, the corrosion characteristics of lead-free solder alloys such as Sn-1.0Ag-0.5Cu- $X$ Zn ( $X= 0, 0.1, 0.5, 1.0$ ) and Sn-1.0Ag-0.5Cu- $X$ Al ( $X=0, 0.1, 0.5, 1.0$ ) have been investigated in 3.5wt-% NaCl solution. The corrosion behavior of were studied through Polarization curve and the Electrochemical Impedance Spectroscopy (EIS) by using Gamry Echem Analyst DC105 software. The microstructure and element of the corrosion compounds formed on the surface of lead-free solder alloys were investigated by Scanning Electron Microscopy (SEM), Energy-dispersive X-ray Spectroscopy (EDX), and X-ray Diffraction (XRD). The polarization curves showed that the addition of Zn in SAC105 solder alloy increased the corrosion current density and shifted the corrosion potential towards more negative values. As a result, the corrosion resistance of Sn-1.0Ag-0.5Cu- $X$ Zn alloys reduces with the increase of Zn concentration. The EIS results agreed well with the findings obtained from polarization curves. The corrosion products at the surface of the investigated Zn doped alloys constituted of  $\text{Sn}_3\text{O}(\text{OH})_2\text{Cl}_2$ , SnO,  $\text{SnO}_2$  and ZnO. Like Zn, addition of Al also decreases the corrosion resistance of the SAC 105 solder alloy.

**Keywords:** corrosion, lead-free solders, EIS, polarization

## KESAN Zn DAN Al TERHADAP CIRI-CIRI KAKISAN ALOI Sn-1.0Ag-0.5Cu

### ABSTRAK

Dalam beberapa tahun kebelakangan ini, aloi pateri timah-plumbum telah popular digunakan dalam industri terutamanya dalam pembungkusan elektronik. Walaubagaimanapun, plumbum dan aloi yang mengandungi plumbum telah disekat penggunaannya dalam industri kerana kebimbangan terhadap alam sekitar dan kesihatan. Baru-baru ini, usaha-usaha telah diambil untuk membangunkan pateri bebas plumbum yang boleh digunakan untuk menggantikan aloi timah-plumbum. Berbanding dengan pateri aloi lain, timah-perak-tembaga (Sn-Ag-Cu) aloi pateri bebas plumbum telah dipilih sebagai alternatif terbaik untuk menggantikan aloi plumbum-timah. Dalam projek ini, tingkah laku kakisan aloi pateri bebas plumbum, Sn-1.0Ag-0.5Cu- $X$ Zn dan Sn-1.0Ag-0.5Cu- $X$ Al ( $X= 0, 0.1, 0.5, 1.0$ ) telah dikaji didalam larutan 3.5wt-% NaCl. Sifat-sifat kakisan aloi pateri bebas plumbum dikaji melalui 'Polarization Curve' dan 'Electrochemical Impedance Spectroscopy (EIS)' dengan menggunakan perisian Gamry Echem Penganalisis DC105. Mikrostruktur dan unsur sebatian karat yang terbentuk pada permukaan aloi pateri bebas plumbum telah dikaji oleh 'Scanning Electron Microscopy (SEM)', 'Energy Dispersive X-ray Spectroscopy (EDX)' dan 'X-ray Diffraction (XRD)'. Hasil kajian menunjukkan bahawa aloi pateri SAC105 mempamerkan ketahanan kakisan yang lebih baik daripada aloi yang mengandungi Zn dan Al. Keputusan 'Polarization curve' menunjukkan dengan menambah Zn ke dalam aloi SAC105 akan meningkatkan 'corrosion current density' dan mengalih 'corrosion potential' ke arah nilai yang lebih negatif. Keputusannya, rintangan kakisan aloi Sn-1.0Ag-0.5Cu- $X$ Zn berkurang dengan penambahan kepekatan Zn. Keputusan 'EIS' selari dengan hasil yang diperolehi daripada 'polarization curve'. Produk kakisan pada permukaan Zn aloi yang didopkan yang telah dikaji membentuk  $\text{Sn}_3\text{O}(\text{OH})_2\text{Cl}_2$ ,  $\text{SnO}$ ,

SnO<sub>2</sub> dan ZnO. Seperti Zn, penambahan Al juga mengurangi rintangan kakisan aloi pateri SAC105.

**Kata kunci:** kakisan, pateri bebas plumbum, EIS, polarisasi

University of Malaya

## ACKNOWLEDGEMENTS

I would like to take this opportunity to express my appreciation to those who have helped and supported me over the past two years. Without them, I would not finish my master program and this dissertation in a smooth manner.

My heart felt thanks to my supervisor, Prof. Dr. A.S.M.A Haseeb and Dr. Mohammad Abul Fazal for their patience, continuous guidance and motivation channeled throughout this research. They were very knowledgeable and dedicated in guiding me and the time spent whenever I faced challenged.

I would like to extent my utmost gratitude to my colleagues, Mrs Nur Suhaila Rosli, Mrs Sundus Fatima, Mrs Fayeka Mansura, Mr Sazzad Sharif for their precious sharing of knowledge, ideas, assistance and fruitful discussions provided to accomplish this research successfully. I would like to express my sincere appreciation to the faculty of engineering, university of Malaya for providing me with all the facilities in the laboratories. Gracious thanks to the dedicated laboratory assistants Mr Nazarul Zaman, Mr Zaharuddin, and others for giving their full co-operation while using the equipment. Special thanks to all the staff of Faculty of Engineering, University of Malaya.

I am grateful for the support provided by University of Malaya' PPP Grant No RP013B-13AET. Last but not least, million thanks to my lovely husband Mohd Syamim Bin Md. Rusli and my family members who gave me full support in making this work a success. Their support and encouragement during times of adversity have made e stronger.

I am also thankful for the effort and contribution shared by individuals whose names are not mentioned above.

Thank you so much.

## TABLE OF CONTENTS

<b>ORIGINAL LITERARY WORK DECLARATION.....</b>	<b>iii</b>
<b>ABSTRACT .....</b>	<b>iii</b>
<b>ABSTRAK.....</b>	<b>iv</b>
<b>ACKNOWLEDGEMENTS.....</b>	<b>vi</b>
<b>TABLE OF CONTENTS.....</b>	<b>vii</b>
<b>LIST OF FIGURES .....</b>	<b>x</b>
<b>LIST OF TABLES.....</b>	<b>xii</b>
<b>LIST OF SYMBOLS AND ABBREVIATIONS.....</b>	<b>xiii</b>
<b>CHAPTER 1: INTRODUCTION .....</b>	<b>1</b>
1.1 Background of Study .....	1
1.2 Objectives.....	3
1.3 Scopes of the study .....	4
<b>CHAPTER 2: LITERATURE REVIEW.....</b>	<b>5</b>
2.1 Introduction .....	5
2.2 Performance characteristics of lead-free solders .....	7
2.2.1 Physical and mechanical properties of solder alloys.....	9
2.2.2 Thermal and electrical properties of solder alloys .....	10
2.2.3 Solder alloy compositions and their functions.....	11
2.2.4 Cost analysis .....	13
2.3 Electrochemical Corrosion Test .....	16
2.3.1 Potentiodynamic Polarization.....	16
2.3.2 Electrochemical Impedance Spectroscopy (EIS .....	18
2.4 Surface characterization techniques.....	18

2.4.1 Scanning Electron Microscopy (SEM) and Energy-Dispersive X-ray Spectroscopy (EDS) analysis .....	19
2.4.2 X-ray Diffraction (XRD) analysis.....	20
2.5 Corrosion behavior of solder alloys.....	21
2.6 Phase diagrams for Sn-Ag-Cu (SAC) solder alloys.....	27
2.7 Microstructure of different alloys .....	29
2.8 Summary and conclusions.....	32
<b>CHAPTER 3: RESEARCH METHODOLOGY .....</b>	<b>34</b>
3.1 Introduction .....	34
3.2 Sample and solution preparation.....	35
3.3 Corrosion test.....	36
3.3.1 Electrochemical test setup .....	37
3.3.2 Potentiodynamic Polarization.....	38
3.3.3 Electrochemical Impedance Spectroscopy (EIS).....	38
3.4 Surface characterization.....	39
<b>CHAPTER 4: RESULTS AND DISCUSSION.....</b>	<b>40</b>
4.1 Introduction .....	40
4.2 Corrosion behavior of Zn-containing solder alloys in 3.5wt-% NaCl solution.....	40
4.2.1 Potentiodynamic polarization curves .....	40
4.2.2 Corrosion rate.....	45
4.2.3 Morphological, elemental and phases analyses of corrosion products .....	45
4.2.4 Electrochemical Impedance Spectroscopy (EIS).....	50
4.3 Corrosion behavior of Al-containing solder alloys in 3.5wt-% NaCl solution .....	52
4.3.1 Potentiodynamic polarization curves .....	52

4.3.2 Corrosion rate.....	57
4.3.3 Morphological, elemental and phases analyses of corrosion products .....	58
4.3.4 Electrochemical Impedance Spectroscopy (EIS).....	61
<b>CHAPTER 5: CONCLUSIONS AND RECOMMENDATIONS.....</b>	<b>64</b>
5.1 Conclusions .....	64
5.2 Recommendations for Future Work:.....	65
<b>REFERENCES .....</b>	<b>67</b>
<b>LIST OF PUBLICATIONS AND PAPERS PRESENTED.....</b>	<b>80</b>

University of Malaysia

## LIST OF FIGURES

<b>Figure 2. 1:</b> Schematic polarization curve of passivable metals .....	17
<b>Figure 2. 2:</b> Schematic EIS Nyquist plots.....	18
<b>Figure 2. 3:</b> Microstructure of the corrosion products on different binary solders after potentiodynamic polarization tests (a) Sn–Ag, (b) Sn–Cu, (c) Sn–Pb (Li et al., 2008) and (d) Sn–Zn (Wu et al., 2006) .....	21
<b>Figure 2. 4:</b> Surface morphology of different ternary solders after potentiodynamic polarization tests: (a) Sn–3.1Ag–0.8Cu, (b) Sn–2.9Ag–6.7Cu, (c) Sn–2.3Ag–9.0In and (d) Sn–3.0Ag–10.4Bi (Rosalbino et al., 2008).....	22
<b>Figure 2. 5:</b> Effect of Al content on the $E_{corr}$ value obtained during polarization of the Sn–8.5Zn–XAl–0.5Ga alloy in 3.5% NaCl solution (Mohanty & Lin, 2006c) .....	24
<b>Figure 2. 6:</b> Effect of the addition of Zn on the corrosion potential and current of Sn–Zn alloys in 6 M KOH (Nazeri & Mohamad, 2014).....	25
<b>Figure 2. 7:</b> X-ray diffraction scans after polarization tests for SAC305 and SAC 105 (Fayeka et al., 2017) .....	27
<b>Figure 2. 8:</b> (a) Ternary phase diagram showing the Sn–Ag–Cu ternary eutectic reaction (Liang et al., 2007; Moon et al., 2000) and (b) Sn-rich corner (Anderson et al., 2001) .....	28
<b>Figure 2. 9:</b> SEM micrographs of different binary solder alloys: (a) Sn–Pb (Wu et al., 2006), (b) Sn–Ag (Glazer, 1994), (c) Sn–Cu (Madeni et al., 2003) (Madeni, Liu, & Siewert, 2003) and (d) Sn–Zn (Wu et al., 2004).....	29
<b>Figure 2. 10:</b> SEM micrographs of different ternary solder alloys: (a) Sn–3.1Ag–0.8Cu, (b) Sn–2.9Ag–6.7Cu, (c) Sn–2.3Ag–9.0In and (d) Sn–3.0Ag–10.4Bi (Rosalbino et al., 2008) .....	31
<b>Figure 3. 1:</b> Flowchart of experimental works.....	35
<b>Figure 3. 2:</b> Sample dimension.....	36

<b>Figure 3. 3:</b> Experimental design for set 1 to set 2 .....	37
<b>Figure 3. 4:</b> Electrochemical setup. ....	38
<b>Figure 4. 1:</b> Potentiodynamic polarization curves of SAC105, SAC105+0.1Zn, SAC105+0.5Zn and SAC105+1.0Zn solder alloys in 3.5wt-% NaCl solution.....	41
<b>Figure 4. 2:</b> SEM micrographs (4600x) of SAC105, SAC105+0.1Zn, SAC105+0.5Zn and SAC105+1.0Zn solder alloys before (a-d) and after (e-h) the corrosion test.....	46
<b>Figure 4. 3:</b> X-ray diffraction scans after polarization for SAC105, SAC105+0.1Zn, SAC105+0.5Zn and SAC105+1.0Zn solder alloys in 3.5wt-% NaCl solution.....	49
<b>Figure 4. 4:</b> Nyquist plot for SAC105, SAC105+0.1Zn, SAC105+0.5Zn and SAC105+1.0Zn solder alloys in 3.5wt-% NaCl solution.....	50
<b>Figure 4. 5:</b> Bode plots (a) Magnitude Bode plot and (b) Phase Angle Bode plot for SAC105, SAC105+0.1Zn, SAC105+0.5Zn and SAC105+1.0Zn solder alloys in 3.5wt-% NaCl solution.....	51
<b>Figure 4. 6:</b> Potentiodynamic polarization curves of SAC105, SAC105+0.1Al, SAC105+0.5Al and SAC105+1.0Al solder alloys in 3.5wt-% NaCl solution.....	53
<b>Figure 4. 7:</b> SEM micrographs (4600x) of (a) SAC105, (b) SAC105+0.1Al and (c) SAC105+1.0Al solder alloys after polarization test.....	58
<b>Figure 4. 8:</b> X-ray diffraction scans after polarization for SAC105, SAC105+0.1Al, SAC105+0.5Al and SAC105+1.0Al solder alloys in 3.5wt-% NaCl solution.....	60
<b>Figure 4. 9:</b> Nyquist plot for SAC105, SAC105+0.1Al, SAC105+0.5Al and SAC105+1.0Al solder alloys in 3.5wt-% NaCl solution .....	61
<b>Figure 4.10 a:</b> Magnitude Bode plot for SAC105, SAC105+0.1Al, SAC105+0.5Al and SAC105+1.0Al solder alloys in 3.5wt-% NaCl solution.....	62
<b>Figure 4.10 b:</b> Phase Angle Bode plot for SAC105, SAC105+0.1Al, SAC105+0.5Al and SAC105+1.0Al solder alloys in 3.5wt-% NaCl solution.....	62

## LIST OF TABLES

<b>Table 2. 1:</b> The main requirements for an alternative solder.....	8
<b>Table 2. 2:</b> Physical and mechanical properties of solder alloys.....	9
<b>Table 2. 3:</b> Thermal and electrical properties of different solder alloys.....	11
<b>Table 2. 4:</b> Properties of alloying element.....	12
<b>Table 2. 5:</b> Approximate price of different elements used in solder alloys.....	14
<b>Table 2. 6:</b> Cost and relative melting temperature ration of some common used lead-free solder alloys.....	15
<b>Table 2. 7:</b> Experimental data of the testing Pb-free solders under polarization in 3.5wt-% NaCl solution.....	26
<b>Table 2. 8:</b> Eutectic temperature and composition of the solder alloys.....	32
<b>Table 4. 1:</b> Potentiodynamic polarization parameters for SAC105, SAC105+0.1Zn, SAC105+0.5Zn and SAC105+1.0Zn solder alloys in 3.5wt-% NaCl solution.....	43
<b>Table 4. 2:</b> Mass percentage of elements present in different alloy surfaces after potentiodynamic polarization test.....	47
<b>Table 4. 3:</b> Electrochemical impedance spectroscopy parameters for SAC105, SAC105+0.1Zn, SAC105+0.5Zn and SAC105+1.0Zn solder alloys in 3.5wt-% NaCl solution.....	51
<b>Table 4. 4:</b> Electrode potential of solder elements.....	54
<b>Table 4. 5:</b> Potentiodynamic polarization parameters for SAC105, SAC105+0.1Al, SAC105+0.5Al and SAC105+1.0Al solder alloys in 3.5wt-% NaCl solution.....	56
<b>Table 4. 6:</b> Mass percentage of elements present in different alloy surfaces after potentiodynamic polarization test.....	59
<b>Table 4. 7:</b> Electrochemical impedance spectroscopy parameters for SAC105, SAC105+0.1Al, SAC105+0.5Al and SAC105+1.0Al solder alloys in 3.5wt-% NaCl solution.....	63

## LIST OF SYMBOLS AND ABBREVIATIONS

$\Delta E$	:	Passivation range
$ Z $	:	Magnitude of impedance
$\theta_{\max.}$	:	Maximum phase angle
$E_{\text{corr.}}$	:	Corrosion potential
$E_{pp.} / E_{\text{pass.}}$	:	Passivation potential
$I_{\text{corr.}}$	:	Corrosion current density
$I_{cc}$	:	Critical current density
$I_{\text{pass.}}$	:	Passivation current density
$R_p$	:	Polarization resistance
Sn	:	Tin
Ag	:	Silver
Cu	:	Copper
Zn	:	Zinc
Al	:	Aluminium
Bi	:	Bismuth
In	:	Indium
Pb	:	Lead
Sb	:	Antimony
Ni	:	Nickel
Au	:	Gold
Ti	:	Titanium
Zr	:	Zirconium
$\text{Cl}^-$	:	Chloride
$e^-$	:	Electron
$\text{H}^+$	:	Hydrogen
$\text{O}_2$	:	Oxygen
$\text{OH}^-$	:	Hydroxide
SnO	:	Tin(II) Oxide
SiC	:	Silicon Carbide

TiO	:	Titanium Oxide
NaOH	:	Sodium Hydroxide
NaCl	:	Sodium Chloride
H <sub>2</sub> O	:	Water
SnO <sub>2</sub>	:	Tin Dioxide
ZnO	:	Zinc Oxide
ZrO <sub>2</sub>	:	Zirconium Dioxide
Al <sub>2</sub> O <sub>3</sub>	:	Aluminium Oxide
Sn(OH) <sub>2</sub>	:	Tin(II) Hydroxide
Sn <sub>3</sub> O(OH) <sub>2</sub> Cl <sub>2</sub>	:	Tin oxide chloride hydroxide
SAC	:	Sn-Ag-Cu
γ	:	Gamma
ζ	:	Zeta
ε	:	Epsilon
IMC	:	Intermetallic Compound
SCE	:	Saturated Calomel Electrode
STEM	:	Scanning/Transmission Electron
EIS	:	Electrochemical Impedance Spectroscopy
SEM	:	Scanning Electron Microscopy
EDS	:	Energy Dispersive x-ray Spectroscopy
XRD	:	X-ray Diffraction
EPMA	:	Electron Microprobe Analysis
TEM	:	Transmission Electron Microscopy
AC	:	Alternating Current
RoHS	:	Reduction of Hazardous Substances
EPA	:	Environmental Protection Agency
WE	:	Working electrode
CE	:	Counter electrode
RE	:	Reference electrode
SCE	:	Saturated calomel electrode
Å	:	Ångström (unit of length)

ml	:	Millilitre
Vol.	:	Volume
lb	:	Pound
t	:	Tan
g	:	Gram
kg	:	Kilogram
mm <sup>2</sup> /s	:	Millimeter square/second
wt. %	:	Weight percentage
T <sub>m</sub>	:	Melting temperature
in <sup>3</sup>	:	Inch cube
W/[m·K]	:	Watts per meter kelvin
J/[kg · K]	:	Joule per kilogram kelvin
°	:	Degree
C	:	Celcius
MPa	:	Mega Pascal
GPa	:	Giga Pascal
mN/m	:	Millinewton per meter
g/cm <sup>3</sup>	:	Gram per centimeter cube
%	:	Percentage
\$	:	Dollar
lb	:	Pounds
V	:	Volt
kV	:	Kilovolt
mA	:	Milliampere
Hv	:	Vickers pyramid number
Hz	:	Hertz
μΩ·cm	:	Microhm centimeter
mV	:	Millivolt
A/cm <sup>2</sup>	:	Ampere per centimeter square

## CHAPTER 1: INTRODUCTION

### 1.1 Background of Study

Solder is a part of an electronic packaging that plays various crucial roles such as electrical and mechanical connections. For a long time in the past, Sn-Pb solders were widely used in the electronic industries because of their low melting temperature, good wettability, low cost, good solderability, good corrosion resistance and satisfactory mechanical properties which are required for interconnecting electronics components (Ahmido et al., 2011; Kar et al., 2007; Richards, 1999). However, due to the new legislations and market driving forces worldwide, recently the use of Pb-containing solders are either severely restricted or completely prohibited. Therefore, different lead-free solder alloys are recently being used to replace Pb-based solder alloys. Availability, corrosion resistance, solderability and mechanical properties could be different for different solder alloys.

Sn-Ag-Cu (SAC) solder family is found to be promising candidate to replace Sn-Pb solders due to its properties such as melting temperature, microstructure, wettability, and interfacial, together with mechanical properties are better than Sn-Pb (Ervina & Amares, 2014; Luo et al., 2005). Additionally, SAC solder is easy to use and appears to be more feasible in terms of cost (Kotadia et al., 2014). Zhang et al. (2012) reported that the eutectic SAC solder could be categorized based on three different compositions proposed by different countries: USA (Sn-3.9Ag-0.6Cu), Europe (Sn-3.8Ag-0.7Cu) and Japan (Sn-3.0Ag-0.5Cu). They reported that SAC solders are not suitable for all applications due to their poor wettability and high melting temperature (227°C). Therefore, addition of various elements such as Zn, Al, In, Bi, Ni and Co seems to produce enhancement on the prior bulk solder alloy (Bashir et al., 2015; Kotadia et al., 2014; Zhang yet al., 2012).

Zinc (Zn) is used as alloying agents in solder alloys because due to its reasonable cost, exhibits better fatigue life and its melting temperature (199°C) which is very close to the conventional eutectic Sn-Pb solder (183°C) (El-Daly et al., 2009). Adding Zn into SAC solder tends to reduce the melting temperature by about 2°C (Ervina & Amares, 2014) and increase the tensile strength (Lin & Chuang, 2010). Kotadia et al. (2012) reported that Cu<sub>3</sub>Sn voids can be suppressed upon addition of Zn and thereby could produce a better joint. Zhang et al. (2012) found that the best amount of Zn to improve the wettability, mechanical properties, thermal fatigue properties and refined the microstructure of SAC solder. However, there is very little information to understand the effect of Zn on the corrosion resistance of the solder alloy.

Aluminium (Al) is also widely used in lead free solder alloys due to its low cost, light weight, high electrical and thermal conductivity (Davies, 2003; Miller et al., 2000; Rana et al., 2012). Wettability of Sn-Cu and Sn-Zn solder alloy can be improve by addition of Al as reported by Lin and Liu (1998b); Lin and Wen (1998); and Yang et al. (2015). Sabri et al. (2013) had studied the microstructural stability of Sn-1Ag-0.5Cu-XAl solder alloy and the effects of high-temperature aging on their mechanical properties, the results revealed that the yield strength, elastic modulus and ultimate tensile strength can be increase by the addition of Al.

Zn well-known as a solder element that is highly susceptible to corrosion and oxidation in the air. The presence of Zn in the solder alloy results in poor corrosion resistance (Mohanty & Lin, 2006b) and becomes important problem to be address. While, Al was used as alloying agents because it can improve the corrosion resistance as reported by Miller et al. (2000) and Davies (2003). However, there is very little information to understand the effect

of Zn and Al on the corrosion resistance of the solder alloy. Some researchers have studied the corrosion behaviour of Sn-Zn-*X* and Sn-Al-*X* solders (Lin et al., 1998; Lin & Liu, 1998a), but fundamental studies on the corrosion properties of Sn-Ag-Cu-Zn and Sn-Ag-Cu-Al solders are rare. Therefore, it is important to study the effect of Zn and Al on the corrosion behaviour of Sn-based solder alloys. In response to that, this study provides detailed information about polarization and electrochemical impedance spectroscopy (EIS) characteristics of Sn-Ag-Cu-Zn and Sn-Ag-Cu-Al alloys in 3.5wt-% NaCl solution.

## 1.2 Objectives

The overall aim of this thesis is to understand the effects of the addition of a fourth element on the corrosion resistance of low cost, low silver Sn-Ag-Cu alloys. This study embarks on the following objectives:

- i. To investigate the effects of addition of zinc on the corrosion behaviour of Sn-1.0Ag-0.5Cu alloys.
- ii. To investigate the effects of addition of aluminium on the corrosion behaviour of Sn-1.0Ag-0.5Cu alloys.
- iii. To examine the surface morphology and damage of the solder alloys after corrosion test.

### 1.3 Scopes of the study

The scopes of the work are as follow:

- i. In this research, the corrosion behavior of Sn-Ag-Cu-Zn and Sn-Ag-Cu-Al alloys in 3.5 wt-% NaCl solution were investigated by Potentiodynamic Polarization test and Electrochemical Impedance Spectroscopy (EIS) test.
- ii. The effect of alloying element was investigated by using different composition of Zinc and Aluminium.
- iii. The composition of corrosion products was evaluated by using a verity of characterization techniques such as scanning electron microscope (SEM), energy dispersive x-ray spectroscopy (EDS), and x-ray diffraction (XRD).

University of Malaya

## CHAPTER 2: LITERATURE REVIEW

### 2.1 Introduction

Solder is a fusible metal alloy with a melting point or melting range of 90 to 450°C (Oberg & Jones, 1988), used in a process called soldering where it is melted to join metallic surfaces. In electronic industry, solder plays an important role on interconnecting and assembling the silicon die (Abteu & Selvaduray, 2000; Richard & Michael, 2004). Soldering interest in microelectronic packaging is increasing because the microelectronic industry has made rapid development in the recent years. Previously Sn-Pb solders were widely used in the electronic industries because of their low melting temperature, good wettability, low cost, good solderability, good corrosion resistance and satisfactory mechanical properties which are required for interconnecting electronics components (Che et al., 2010; Garcia et al., 2010; Osorio et al., 2011). Lead-free solder alloys have been needed to replace the Pb-Sn solders as the primary interconnecting materials in electronic packaging due to the drive for green electronic products. Lead was banned effective in July 1, 2006 by European RoHS (Reduction of Hazardous Substances) (Osorio et al., 2014). The US EPA (Environmental Protection Agency) has also expressed concern on usage of lead due to the appearance toxicity of Pb and solders containing Pb (Abosheiasha et al., 2012).

In the electronics industry, efforts are now being made to develop a usable lead-free solder. An alternative solder alloys must meet satisfactory properties in order to replace Pb-containing solder alloys. Several tin-based alloys have already been proposed to replace Sn-Pb solder alloys such as binary system Sn-Ag, Sn-Cu, Sn-Zn, etc. and ternary system such as Sn-Ag-Cu, Sn-Zn-Ag, Sn-Zn-In based solders (Abosheiasha et al., 2012; Gouda & Aziz, 2012; Osório et al., 2014). Sometime the properties of the binary or ternary Pb-free solders

cannot fully meet the requirements for applications in electronic packaging and therefore additional alloying elements are added to improve the performance of these alloys. Several researchers found that addition of alloying elements such as Cu, Ag, Zn, Bi, In, etc. into Sn-based alloy can serve as a new Pb-free solder with better properties. The properties of the lead-free solders required into the modern electronics industry includes low melting points, good wettability, good corrosion resistance, low cost, reasonable electrical conductivity, and satisfactory mechanical properties (Che et al., 2010). Since the Sn-rich solders are considered to be among the best lead-free alloys, many researches have been made on their properties, microstructures and cost as well (Hassam et al., 1998; Huang & Wang, 2005; Kim et al., 2003; Kumar et al., 2006; Schaefer & Lewis, 2005). It is noted that the melting point and wettability are the key properties as the current technologies are based upon those of Sn-Pb. From literatures, it has been found that the addition of alloying elements as well as nanoparticles in Sn-rich solders can improve its properties and structural stability (Chuang et al., 2011; Shen et al., 2006; Tsao et al., 2010).

For achieving high reliability, solder materials should also have good corrosion resistance. In general, solder alloys ensure electric connection with different metallic components in the electronic device and thus, it could introduce galvanic corrosion at the joints of two different metals. This could be further exacerbated when the electronics are exposed to a variety of outdoor and indoor environments. The corrosion characteristics of the environments are mostly influenced by humidity, temperature, pollutants, etc. (Andersson & Liu, 2008). When solder joints or soldered components are affected by corrosion, it could change the microstructure of the corroded regions and introduce crack initiation sites. Thus, it may alter the physical, mechanical and electrical properties of the joints. The alteration of the properties of the lead-free solder alloys in corrosive environments has not

been widely reported, although it is important for many automotive, marine, aerospace and defense applications (Li et al., 2008).

The development of lead-free solders has become an important mission for materials scientists due to the drive for green electronic products (Gouda & Aziz, 2012). It is very important to ensure that the properties of an alternative solder alloy are comparable to or superior than those of Sn-Pb solders. In order to be an excellent replacement solder for Pb-containing solder, there are strict performance characteristics that must be fulfilled. In general, the solder alloys not only must meet expected levels of physical and mechanical properties such as melting point, density, tensile strength, yield stress, etc., but they also should performed good electrical and thermal properties such as thermal diffusivity, electrical resistivity, thermal conductivity, etc. However, it is difficult to obtain specific information regarding these properties. In response to this, the present study attempts to gather all the necessary data and information of solder alloys from the recent literatures. Data to be generated are expected to resolve some problems related to the improvement of the reliability of lead-free solder alloys.

## **2.2 Performance characteristics of lead-free solders**

In microelectronics, performance of new solder is an important requirement that must be fulfilled when trying to identify the best replacement to the current Pb-Sn solder. It is a big responsibility to ensure that the characteristics of the alternative solder are comparable to or superior than Pb-containing solders. In that case, the final decision to be taken could be dominated by some performance measuring parameters shown in Table 2.1. The required properties include low melting temperature ( $T_m$ ), good wettability, good creep resistance,

low electrical resistivity, high thermal conductivity, improved coefficient of thermal expansion etc.

**Table 2. 1:** The main requirements for an alternative solder.

Parameters	Requirements	Descriptions	References
Physical and mechanical properties	Low melting temperature ( $T_m$ )	$T_m$ of SnPb is 183°C but it is significantly higher for some lead-free solder alloys. Increased $T_m$ can degrade the components, soldering flux or paste chemistry, attach materials.	(Kotadia et al., 2014; Lee et al., 2005; Noh et al., 2010; Puttlitz & Stalter, 2004; Yamamoto & Tsubone, 2007)
	Good wettability		
Thermal and electrical properties	High tensile strength	Other properties are similar or better than those of SnPb.	
	Good creep resistance		
	Low electrical resistivity	Exhibit similar or better than those of SnPb alloy.	
	High thermal conductivity		
	Improved coefficient of thermal expansion		

Table 2.1 indicates that all the listed parameters except melting temperature exhibit similar or better properties than those of SnPb solder alloys. Therefore, the melting temperature could be the most important factor to find the best alternative lead-free solder alloys. It must exhibit similar or better than lead solder alloy because high melting temperatures can give effect on components, soldering flux or past chemistry, cleaning and substrate material properties. For higher melting points solder alloy, longer contact period between the solder and the connections is required for solder to completely fill the holes (Subramanian, 2007).

Besides, lead-free solder alloys must exhibit good wettability. Wettability is the tendency of a liquid to disseminate over a solid substrate. Contact angle and surface energy of the interface will affect the degree of wetting. Whereas, the rate of wetting will influence the ability of liquid wet the surface and spreads over the substrate. Therefore, in order to ensure the bond between the base metal and solder was formed, solder alloys must wet the base

metal properly by purpose a good wettability (Wu et al., 2004). In addition to the melting point and wettability, the other parameters to measure the performance of the lead-free solder alloys include tensile strength, electrical resistivity, thermal conductivity, density etc. All the data for these properties are discuss in next section.

### 2.2.1 Physical and mechanical properties of solder alloys

The physical and mechanical properties of solder alloys such as melting point, density, tensile strength, yield stress and etc. are an important index to evaluate solder properties. It plays a vital role in the reliability of solder joints. The comparison data between lead-containing and lead-free solder alloys are summarized in the Table 2.2 below:

**Table 2. 2:** Physical and mechanical properties of solder alloys.

	Sn-Pb	Sn-Ag	Sn-Ag-Cu	Sn-Ag-Bi	Sn-Zn-Al
Melting point (°C)	183	221	218	138	199
Density (g/cm <sup>3</sup> )	8.5	7.5	7.4	8.6	7.3
Surface tension (mN/m)	420	-	450 - 500	380 – 390	518
Young's modulus (GPa)	22	56	31	24	36
Poisson's ratio	0.37	-	0.4	0.43	0.44
Tensile strength (MPa)	41	61	35	60	46
Shearing strength (MPa)	27	32	30	36	32
Yield stress	28	23	27	35	27
Elongation (%)	38	35	23	40	25
Vickers hardness (Hv)	13	-	15	15	19
Reference	(Yamamoto & Tsubone, 2007)	(Smith et al., 2002)	(Bilek et al., 2006; Yamamoto & Tsubone, 2007)	(Puttlitz & Stalter, 2004; Yamamoto & Tsubone, 2007)	(Yamamoto & Tsubone, 2007)

Among the various binary alloy systems, Sn-Ag solder is found as one of the earliest commercially available lead-free solders which provide better mechanical properties than

those of Sn-Pb solder (Huang et al., 2012; Kariya & Otsuka, 1998). However, the high melting temperature of Sn-Ag (221°C) has limited its application on the current manufacturing technologies and base on the current Sn-Pb (183°C). From Table 2.2, it is seen that addition of copper, bismuth can depress the melting point of Sn-Ag based solders. Sn-Zn-Al could be another alternative solder which has very close melting temperatures to that of Sn-Pb but it seems brittle along with high hardness value (19Hv). Recently doping with nano-sized, non-reacting, non-coarsening, oxide disper solders (e.g. TiO<sub>2</sub>, Al<sub>2</sub>O<sub>3</sub>, ZrO<sub>2</sub>, etc.) have been identified in improving mechanical properties as well as microstructural stability (Chuang et al., 2011; Shen et al., 2006; Tsao & Chang, 2010; Tsao et al., 2010).

### **2.2.2 Thermal and electrical properties of solder alloys**

For many years, when the microelectronics device is functioning, a primary method of establishing mechanical and electrical connections in electronic is by soldering. While there are several electrical and thermal properties of solders that are of interest to the electronics community at large, most significant properties to an engineer are thermal conductivity, specific heat, thermal diffusivity, electrical resistivity and coefficient of thermal expansion as listed in the Table 2.3 below. An alloy of tin, silver and copper termed SAC is the best candidate to replace tin-lead (Sn-Pb) solder. From Table 2.3, it is seen that properties exhibited by the SAC alloys is closest to the Sn-Pb alloys as compared with other lead-free solders. It is observed that each thermal and electrical property of SAC solder is very close to that of Sn-Pb solders.

**Table 2. 3:** Thermal and electrical properties of different solder alloys.

	Sn-Pb	Sn-Ag	Sn-Ag-Cu	Sn- Ag-Bi	Sn-Zn-Al
Coefficient of thermal expansion ( $10^{-6}/^{\circ}\text{C}$ )	24	20	21	15	23
Specific heat ( $\text{J}/[\text{kg} \cdot \text{K}]$ )	197	-	234	170	243
Thermal conductivity ( $\text{W}/[\text{m} \cdot \text{K}]$ )	50	55	55	21	66
Thermal diffusivity ( $\text{mm}^2/\text{s}$ )	30	-	31	14	37
Electrical resistivity ( $\mu\Omega \cdot \text{cm}$ )	15	12	11	12	34-58
Reference	(King, 1988; Yamamoto & Tsubone, 2007)	(Paul, 2010; Smith et al., 2002)	(Paul, 2010; Yamamoto & Tsubone, 2007)	(Yamamoto & Tsubone, 2007)	(Yamamoto & Tsubone, 2007)

### 2.2.3 Solder alloy compositions and their functions

Different elements serve different roles in the solder alloy. Tin (Sn), silver (Ag), copper (Cu), zinc (Zn), nickel (Ni), bismuth (Bi), indium (In) and antimony (Sb) are the alloying elements used in commercial lead-free solders. Sn-based multi-component alloys with addition of these alloying elements are likely to be the most potential candidate to substitute the conventional Sn-Pb solder because of their satisfactory properties.

Tin (Sn) is the usual main structural metal of the alloy. It has good strength and wetting. Formation of Kirkendall voids can be prevented by the presence of silver. Silver (Ag) provides mechanical strength, but has worse ductility than lead. In absence of lead, it improves resistance to fatigue from thermal cycles (Kostov et al., 2009). Takemoto et al. (1999) reported that the wettability of Sn-9Zn can be approved by the addition of Ag as well as its oxidation resistance. Addition of silver to tin significantly lowers solubility of silver coatings in the tin phase.  $\text{Ag}_3\text{Sn}$  platelets tend to form in eutectic Sn-3.5Ag alloy,

which, if formed near a high-stress spot, may serve as initiating sites for cracks. Therefore to avoid such issue, silver content needs to be kept below 3% (Tu, 2007).

Copper (Cu) are capable of lowering the melting point, improves resistance to thermal cycle fatigue, and improves wetting properties of the molten solder (Salimin, 2008). Rosalbino et al. (2008) revealed that the corrosion resistance was significantly improved by the addition of Cu from 0.8 to 6.7 at%. Addition of copper may also lead to the formation of intermetallic compounds and may promote growth of tin whiskers.

**Table 2. 4:** Properties of alloying element.

Element	Properties			References
	Corrosion resistance	Melting point	Wettability	
Sn	Good	-	Good	(Xu et al., 2006)
Ag	Good	Lowers	-	(Rosalbino et al., 2008)
Cu	Good	Lowers	Improves	(Rosalbino et al., 2009)
Zn	Poor	Lowers (Closed to Sn-Pb)	-	(El-Daly & Hammad, 2010)
Bi	Good	Lowers	Improves	(Choi et al., 2002)
In	Poor	Lowers	Lowers	(Puttlitz & Stalter, 2004)

Zinc (Zn) was used as alloying agents in solder alloys because it is cheaper, exhibit better fatigue life and its melting temperature (199°C) is very closed to conventional eutectic Sn-Pb solder (183°C) (El-Daly et al., 2009). However it is highly susceptible to corrosion and oxidation in air (Cheng & Lin, 2005; McCormack & Jin, 1993; Song & Wu, 2006; Suganuma et al., 2011). Therefore zinc-containing alloys are unsuitable for some purposes.

Low melting point element; Bismuth (Bi), can significantly lowers the melting point, improves wettability and enhances its adhesion strength on the Cu substrate (Liu et al., 2007). Zhou et al. (2005) reported that Bi-containing alloys were also found to be rather to corrosion and oxidation. However this alloying element relatively expensive and limited availability (Bastecki, 1999).

Indium (In) is a useful element to solve the problem of high melting temperature and it can improve the ductility (Yu et al., 2000). In presence of lead it forms a ternary compound that undergoes phase change at 114 °C. However, Indium is expensive (several times of silver) and low availability. In the presence of chloride ions, Indium-based solders are prone to corrosion (Walker, 2011).

It can be conclude that Sn, Ag and Cu can increased the corrosion resistance of the solder, while the corrosion resistance of the alloys was decreased with the addition of Zn and In. Besides, effect on melting point and wettability were also important when choosing the alloying elements to substitutes the traditional Sn-Pb solder.

#### **2.2.4 Cost analysis**

Till date, the electronic industry has examined a good number of alloy systems alternatives to Sn-37Pb solder. It appears that most of the favored direction is leading towards Sn-Ag-Cu for replacing Sn-Pb solder. Any replacement alloy to be chosen should be economical along with meeting other the functional requirements. Unfortunately lead is relatively inexpensive and none of the replacement alloy is economical. Several alternative lead-free solder systems are quite interesting from technical standpoint but seem unsatisfactory when considering the availability, cost, reliability and repeatability of manufacture. Technically

Sn-3.5Ag-0.5Cu alloy seems almost fit to replace 63Sn/37Pb and in this case, 37% Pb is altered by 3.5% Ag, 0.5%Cu.

**Table 2. 5:** Approximate price of different elements used in solder alloys

Elements	Cost, \$ per Pound (As of 7/2/17)	Cost, \$ per pound (As of 2/3/99)	Cost ratio	Availability
Pb	3.29	0.45	7.3	-
Sn	12	3.50	3.4	Available
Ag	283	84.20	3.4	Available
Cu	9	0.65	14	Available
Zn	1.47	0.50	3	Available
Ni	18	-	-	Available
Al	3.53	-	-	Available
Sb	12	0.80	15	Available
Bi	23	3.4	6.8	Available
In	318	125.00	1.5	Scare
Reference	(JM Bullion; Rotometals)	(Bastecki, 1999)		

Table 2.5 shows the approximate price of different elements used in solder alloys. It is seen that all of the three elements, Ag, Cu and Sn are more expensive than Pb. It is also seen that per pound Pb costs only 3.29\$ while the costs of alternative elements including Cu, Ag, In are 9, 283 and 318\$ respectively. Zn is the cheapest alternative metal but it easily forms IMCs at the joint by making it brittle and also causes corrosion (Hammad, 2013; Rosalbino et al., 2008; Smith et al., 2002; Yamamoto & Tsubone, 2007). As mentioned above, 9% Zn could be alloyed with Sn only upon addition of either Ni (Billah et al., 2014), Bi (Kim et al., 2005; Shih & Lin, 2011; Shohji et al., 2004) or Ag (Takemoto et al., 1999). Additionally, the price of these elements increased at different rate with time. It is seen that within 18 years starting from 1999 to 2017, the price of copper has been increased 14 times

while it is only 1.5 times for In (Table 2.5). The industry will certainly consider these factors for selecting the best alloy composition suited for the broadest range of applications.

**Table 2. 6:** Cost and relative melting temperature ration of some common used lead-free solder alloys

Solder alloys	Cost (US\$)/ Ib	Relative cost Ratio 63Sn/37Pb=1	Relative T <sub>m</sub> Ratio 63Sn/37Pb=1
63Sn/37Pb	2.37	1	183/183 = 1
96.5Sn/ 3.5Ag	6.32	2.7	221/183 = 1.2
95.5Sn/4Ag/0.5Cu	6.55	2.76	218/183=1.19
93.5Sn/3.5Ag/3Bi	5.92	2.5	138/183=0.75
77.2Sn/20In/2.8Ag	30.06	12.7	186/183=1.02
91.8Sn/3.4Ag/ 4.8B	6.24	2.6	215/183=1.17
91Sn/9Zn	3.23	1.36	199/183=1.09
96.2Sb/2.5Ag/0.8Cu/0.5Sb	5.48	2.31	219/183=1.19
95Sn/3.5Ag/1.5In	8.15	3.4	218/183=1.91
Reference	(Bastecki, 1999; Lee et al., 1995; Puttlitz & Stalter, 2004)	(Bastecki, 1999)	

Table 2.6 represents the cost and relative temperature ratio for several lead free solder alloys. It is seen that the lead-free solders are more expensive than the Sn-37Pb solder. However, Sn-9Zn seems to be the most reasonable alloy in terms cost and low melting temperature. But Zn made solder is subjected to corrosion and oxidation (Billah et al., 2014; Hammad, 2013; Rosalbino et al., 2008; Smith et al., 2002; Yamamoto & Tsubone, 2007) and therefore, Sn-Zn cannot be best alternative in replacing Pb-Sn solder alloy. Till today, many researchers have been conducted to find the best alternative to Sn-Pb (Guo et al., 2003; Guo et al., 2001; See et al., 2016; Xu et. al., 2011; Yao et al., 2008). Among others, Sn-Ag-Cu seems to be most promising one as it has low cost and low melting point.

### 2.3 Electrochemical Corrosion Test

Electrochemical corrosion tests can provide valuable information about corrosion process and mechanism. The most common methods used for the study of corrosion of alloys are Potentiodynamic Polarization and Electrochemical Impedance Spectroscopy (EIS). These two methods are briefly described as follows ("Basics of Electrochemical Impedance Spectroscopy,"; "Lecture 11: Electrochemical Techniques,").

#### 2.3.1 Potentiodynamic Polarization

Polarization methods mean changing the working electrode potential and measure the reaction rate, which is the current produced as a function time or potential. Polarization curves are particularly valuable in determining the behaviour of materials under various conditions. Fig. 2.1 shows a typical schematic diagram of cathodic and anodic scans in general with active, passive and transpassive region. The scan starts at 1 and end at 2 with increasing in potential. AB and BG represent cathodic and anodic behaviour respectively. AC and DC denote Tafel-type straight lines corresponding to reduction of hydrogen evolution ( $2\text{H}^+ + e = \text{H}_2$ ) and oxidation reaction of the normal metal dissolution ( $\text{M} = \text{M} + e$ ).

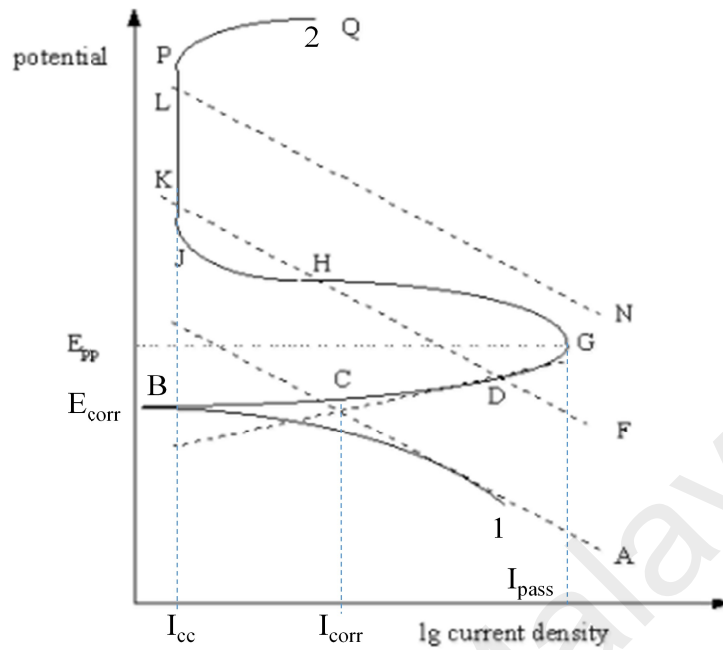


**Figure 2. 1:** Schematic polarization curve of passivable metals

The corrosion rate of the system is represented by corrosion-current density,  $I_{corr}$  at intersection point C of Tafel lines. As the potential increases more positive than  $E_{corr}$ , the corrosion rate keeps increasing until it reaches a maximum at point G, wherein passive potential and critical current density is often given the symbol  $E_{pp}$  and  $I_{cc}$  respectively. At point G, formation of protective film begins and causes a sudden drop in corrosion current density in the region G to J. The passive current density,  $I_{pass}$  is maintained at a steady low level at passive zone of JP until at point P; breakdown of the protective film begins. At potentials more positive than P, the curve runs into transpassive region PQ, and the current density suddenly increases due to some factor such as propagation of pits.

### 2.3.2 Electrochemical Impedance Spectroscopy (EIS)

Electrochemical impedance spectroscopy (EIS) is an Alternating Current (AC) Test which is used for characterizing a wide variety of electrochemical systems. One of the main advantages of this technique is the ability to assess the degradation of metals. Fig. 2.2 illustrated the schematic EIS Nyquist plots for measuring the corrosion process.

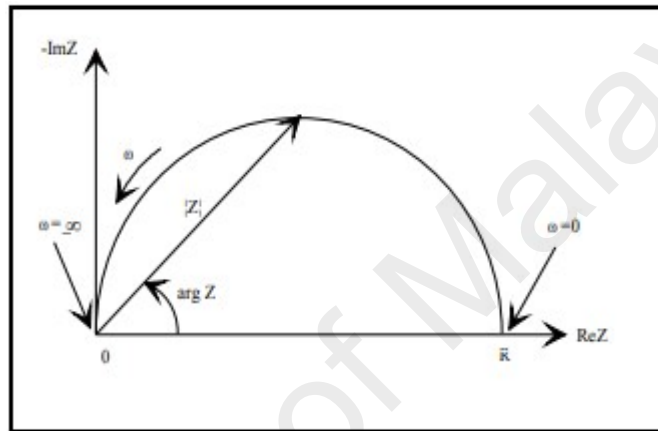


**Figure 2. 2:** Schematic EIS Nyquist plots

The principle of this technique is to apply an AC of small amplitude to an electrode inserted into an electrolyte and measuring the response current through the cell. The impedance is expressed as complex number  $Z(\omega)=Z_0(\cos \Phi + j\sin \Phi)$ . If the real part is plotted on the X axis and the imaginary part on the Y axis of a chart, a Nyquist plot can be obtained like that in Fig. 2.2 with high frequencies on the left and low frequency on the right.

### 2.4 Surface characterization techniques

The surface characterization techniques have established their importance in many areas such as scientific, industrial, and commercial (Brundle et al., 1992; Buckley, 1981; Glaeser, 2010; Kinloch, 1982; Miyoshi & Chung, 1993; Quinn, 1991). This is because the surface

plays a significant role in many thermal, chemical, physical, and mechanical processes. The most common useful tool available today in studying the morphology, defects, and wear behavior of material surfaces are scanning electron microscope (SEM), Energy-Dispersive X-ray Spectroscopy (EDS) analysis and X-ray Diffraction (XRD) analysis.

#### **2.4.1 Scanning Electron Microscopy (SEM) and Energy-Dispersive X-ray Spectroscopy (EDS) analysis**

SEM is basically known as a unique tool for microstructural studies. It produces images of solid material surfaces in large depth of field over a wide range of magnifications. This makes SEM one of the most extensively used instruments in this research area today. SEM uses electrons instead of light to form images of the metal surfaces. A beam of electrons is produced at a microscope by heating of a metallic filament. The electron beam normally follows a vertical path through the column. It makes its way through electromagnetic lenses at the microscope and then focus and directs the beam down towards the sample. Once it hits the sample other electrons are ejected from the sample. However, not all of the electrons are detected and used for information. Detectors collect the secondary or backscattered electrons only. Then it converts them to a signal that is sent to a viewing screen, which produces an image. This processing has to be done in vacuum otherwise the transmission of the beam through the electron optic column could be delayed by the presence of other molecules.

A SEM analysis presents 2D-images of the metals samples. It is also possible to differentiate the different depth range by the light of the backscattered and secondary electrons, and chemical analysis, by means of energy dispersive X-ray spectroscopy analysis

(EDS). In this thesis, the SEM analysis were performed using Phenom Pro X SEM Tabletop equipped with an energy dispersive spectroscopy X-ray (EDS) analysis system.

#### **2.4.2 X-ray Diffraction (XRD) analysis**

X-rays increase in energy as the wavelengths of the light is decreases. X-rays have high energy and they are electromagnetic with the wavelength is almost same size as an atom, which is about  $1 \text{ \AA}$  ( $10^{-10} \text{ m}$ ). Different amount of radiation were let pass from different materials which has different densities. Dense materials are seen as dark shadows since they absorb more X-rays. Meanwhile, lighter materials are lighter in contrast because they let pass more X-rays. The X-ray machine has a quite simple principle. X-ray tube are available inside the machine. High energy electrons was shoots at a target by electron gun inside the X-ray tube which is made of heavy atoms such as tungsten. High energy electrons that were shot at the target induced an atomic de-excitation process and cause X-rays to come out. X-ray photons can be produce by two different atomic processes. The first atomic process is called Bremsstrahlung where after swinging around the nucleus of a tungsten atoms, the electrons were slow down and loses energy by radiating x-rays. A lot of photons are in reality produced, but none of the photons has more energy than the electron had to begin with. The original electron is slowed down or stopped after emitting the spectrum of x-ray radiation. K-shell emission is the second atomic process where the sufficient energy given by the incoming electron from the electron gun knocked K-shell electron in a tungsten target atoms, and a tungsten electron of higher energy (from an outer shell) can fall into the k-shell. In an emitted x-ray photon, the energy lost by the falling electron was arise. Meanwhile, higher energy electrons fall into the vacated energy state in the outer shell, and so on. Higher intensity x-rays was produces by K-shell emission as compared to Bremsstrahlung, and the x-ray photon comes out at a single wavelength.

Both ways involve a change in the state of the electrons. In this work, PANalytical EMPYREAN machine was used and their images were obtained at 40 mA, 45 kV.

## 2.5 Corrosion behavior of solder alloys

The solder connection can be exposed directly not only to the corrosion media such as moisture but also air, oceanic environments, air pollutants from industry, and other corrosives such as chlorine and sulphur compounds rely on their applications. In order to have a long-term reliability, the ability of the solder to withstand such corrosion media is therefore becomes an important factor (McCormack & Jin, 1994). Although lead-free solders alloy is importance in many aerospace, automotive, defense and maritime applications, however, the properties of these alloys in corrosive environments has not been widely reported.

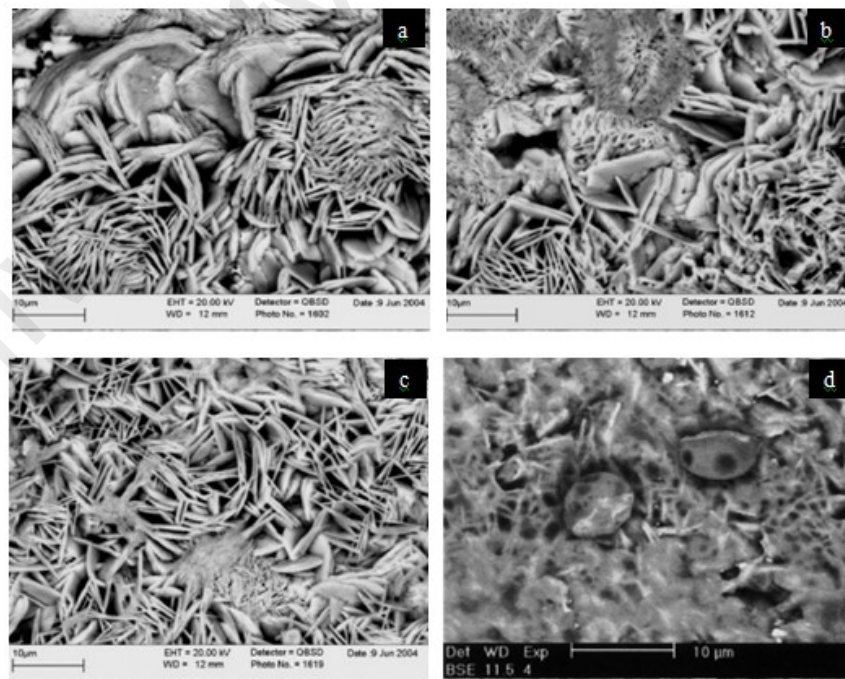


**Figure 2. 3:** Microstructure of the corrosion products on different binary solders after potentiodynamic polarization tests (a) Sn–Ag, (b) Sn–Cu, (c) Sn–Pb (Li et al., 2008) and (d) Sn–Zn (Wu et al., 2006)

Li et al. (2008) has investigated the corrosion behaviour of Sn-Cu and Sn-Ag solders in 3.5-wt.% NaCl solution and compared with that eutectic Sn-Pb solder. Due to the lower passivation current density, lower corrosion current density after the breakdown of passivation film and a more stable passivation film on the surface, lead-free solder exhibits better corrosion resistance than Sn-Pb solder. These results were in accordance with the result obtained by Chang et al. (2004) when they studied the electrochemical behaviors of Sn-Ag, Sn-Zn and Sn-Pb solders in 3.5wt-% NaCl solution.

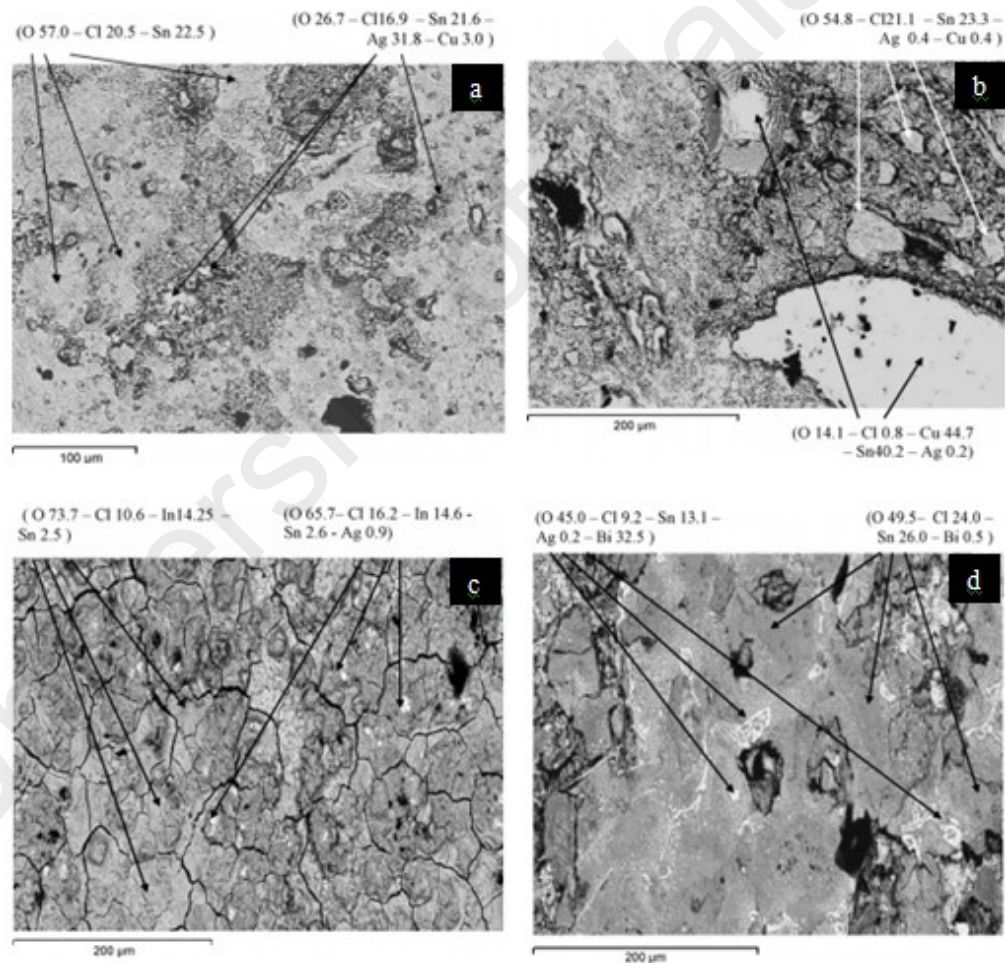


**Figure 2. 4:** Surface morphology of different ternary solders after potentiodynamic polarization tests: (a) Sn-3.1Ag-0.8Cu, (b) Sn-2.9Ag-6.7Cu, (c) Sn-2.3Ag-9In and (d) Sn-3.0Ag-10.4Bi (Rosalbino et al., 2008)

Rosalbino et al. (2008) had studied the corrosion behavior assessment of lead-free Sn-Ag-M (M=In, Bi, Cu) solder alloys. Fig. 2.4 shows the surface morphology of different ternary solders after polarization tests. The corroded surface morphology of the Sn-3.1Ag-0.8Cu solder alloy is shown in Fig. 2.4a. The surface was covered by some narrow pits which spread uniformly. Tin oxychlorides was found at the grey areas while silver enrichment was marked at the light ones. Ag<sub>3</sub>Sn intermetallic compound is retained after the polarization test. Hence, the Ag<sub>3</sub>Sn is more noble than the βSn phase, it does not dissolve during the test but acts as a cathode. On the other hand, the pit was formed due to the reaction between Cl<sup>-</sup> ions and βSn phase which acts as anode in the electrochemical reaction. Fig. 2.4b show the corroded surface morphology of the Sn-2.9Ag-6.7Cu solder alloy. As can be seen, the corrosion attack appears to be less accentuated than the Sn-3.1Ag-0.8Cu solder alloy. Corrosion attack mainly localized at the βSn phase with the formation of grey phase (tin oxychloride) as corrosion products, while white phase (Cu<sub>6</sub>Sn<sub>5</sub> intermetallic compound) remains almost unattacked. Hence, the Cu<sub>6</sub>Sn<sub>5</sub> phase acts as a cathode thus promoting dissolution of the βSn phase in the electrochemical reaction. Fig. 2.4c shows the surface morphology of the Sn-2.3Ag-9.0In solder alloy at the end of a polarization test. The result revealed that a thick layer of corrosion products spread uniformly over the surface with a large number of pits, cracks and other defects. Besides, some white irregular shaped particles are particularly silver-rich and the compound may be Ag<sub>3</sub>Sn were scattered non-uniformly over the surface. The corroded surface morphology of the Sn-3.0Ag-10.4Bi solder alloy as reported in Fig. 2.4d exhibits several pits randomly distributed over the surface and attributable to the dissolution of the βSn phase during the anodic polarization. At the sample surface, significant amounts of grey phase (tin oxychlorides), light phase (bismuth) and dark phase (silver) were detected. This suggests that tin-rich phase protect the Bi-rich phase and the Ag<sub>3</sub>Sn intermetallic compound. As a consequence, the βSn phase

dissolution is accelerated owing to the galvanic action of bismuth and silver, thereby explaining the poor electrochemical behavior shown by the Sn-2.3Ag-9In solder alloy.

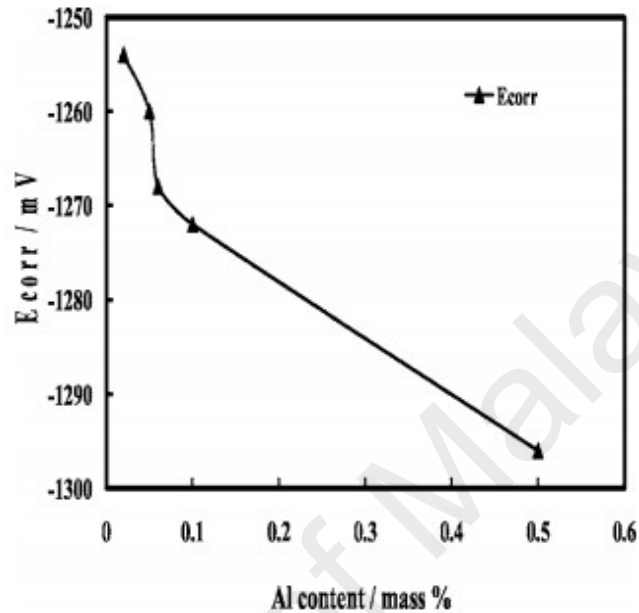


**Figure 2. 5:** Effect of Al content on the  $E_{corr}$  value obtained during polarization of the Sn–8.5Zn–XAl–0.5Ga alloy in 3.5% NaCl solution (Mohanty & Lin, 2006c)

Mohanty and Lin (2006c) had conducted the potentiodynamic polarization measurement on Sn-8.5Zn-XAl-0.5Ga alloy in 3.5% NaCl solution. Fig. 2.5 shows the effect of Al content on the  $E_{corr}$  value obtained during polarization of the Sn–8.5Zn–XAl–0.5Ga alloy in 3.5% NaCl solution. The addition of Al content from 0.02 to 0.5wt% in the Sn–8.5Zn–XAl–0.5Ga alloy shifts the corrosion potential toward more negative values as shown in Fig. besides, the corrosion current density ( $I_{corr}$ ) was increased rapidly with the addition of Al. These results were in accordance with the study conducted by Despic et al. (1976) while investigating the electrochemical behavior of aluminium alloys in the presence of small amounts of gallium and indium. Therefore, the addition of Al decreased the corrosion resistance.

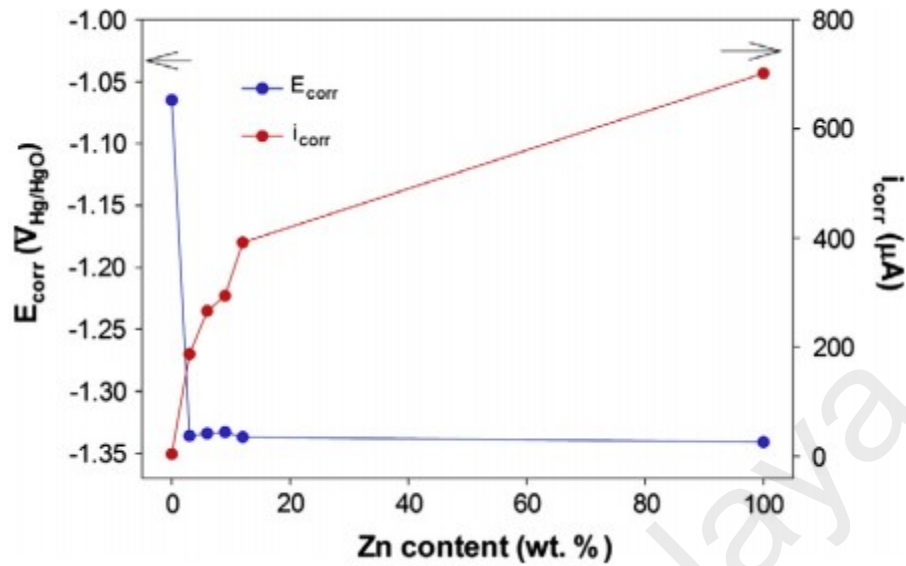


**Figure 2. 6:** Effect of the addition of Zn on the corrosion potential and current of Sn–Zn alloys in 6 M KOH (Nazeri & Mohamad, 2014)

Nazeri and Mohamad (2014) had studied the corrosion measurement of Sn-Zn lead-free solders in 6M KOH solution. Fig. 2.6 shows the effect of the addition of Zn on the corrosion potential and current of Sn–Zn alloys in 6 M KOH. The addition of Zn content in Sn-Zn alloys enhances the corrosion current density ( $I_{corr}$ ) which is corresponding to the increasing of corrosion rate. These happened because Zn is more electrochemically active than Sn, hence acts as anode. As a stronger reducing agent, Zn loses the electron and has been oxidized. The oxidation of the reducing agents causes Zn to become corroded. Therefore, Zn enhances the corrosion.

**Table 2. 7:** Experimental data of the testing Pb-free solders under polarization in 3.5wt-% NaCl solution

Solder	$E_{corr}$ (mV)	$I_{corr}$ (A/cm <sup>2</sup> )	$E_p$ (mV)	$I_p$ (mA/cm <sup>2</sup> )	References
	-576	$7.4 \times 10^{-8}$	-	4.17	(Li et al., 2008)
Sn-37Pb	-1100	$1.11 \times 10^{-3}$	-	-	(Chang et al., 2004)
	-588	$1.905 \times 10^{-6}$	-201	4.989	(Wu et al., 2006)
Sn-0.7Cu	-688	$1.78 \times 10^{-7}$	-	0.74	(Li et al., 2008)
	-705	$4.9 \times 10^{-8}$	-	0.49	
Sn-3.5Ag	-440	$7.52 \times 10^{-2}$	-	3.02	
	1430	$1.07 \times 10^{-1}$	-	10.9	(Li et al., 2008)
Sn-9Zn	-940	$2.691 \times 10^{-5}$	-326	2.938	
Sn-3.5Ag-0.5Cu	-605	$5.370 \times 10^{-7}$	-236	4.083	
Sn-3.8Ag-0.7Cu	-727	$8.9 \times 10^{-8}$	-	1.07	(Li et al., 2008)
Sn-9Zn-0.5Ag	1070	$8.54 \times 10^{-2}$	-	3.92	(Chang et al., 2004)
Sn-8Zn-3Bi	-1291	$1.380 \times 10^{-5}$	9	8.035	
Sn-3.5Ag-0.5Cu-9In	-578	$7.413 \times 10^{-6}$	-158	1.524	(Wu et al., 2006)

$E_{corr}$  – corrosion potential,  $I_p$ – passivation current density,  $I_{corr}$  – corrosion current density,  $E_p$  – passive potential.

As reported by many researchers (Table 2.7) (Chang et al., 2004; Rosalbino et al., 2008; Wu et al., 2006), lead-free solder alloys exhibits better corrosion resistance than Pb-containing solder and corrosion products formed on lead-free solders after electrochemical corrosion test mostly was tin oxide chloride hydroxide ( $\text{Sn}_3\text{O}(\text{OH})_2\text{Cl}_2$ ). This is consistent with the results obtained by Fayeka et al., (2017) when studied the electrochemical corrosion behaviour of Pb-free SAC105 and SAC305 solder alloys. Fig. 2.7 shows X-ray diffraction scans after polarization tests for SAC305 and SAC 105.  $\text{Sn}_3\text{O}(\text{OH})_2\text{Cl}_2$ ,

$\text{Sn}_3\text{O}_2(\text{OH})_2$ ,  $\text{SnO}_2$ ,  $\text{SnO}$ ,  $\text{Cu}_6\text{Sn}_5$  and  $\text{Ag}_3\text{Sn}$  are the phases that are detected at the exposed surface during the scan.

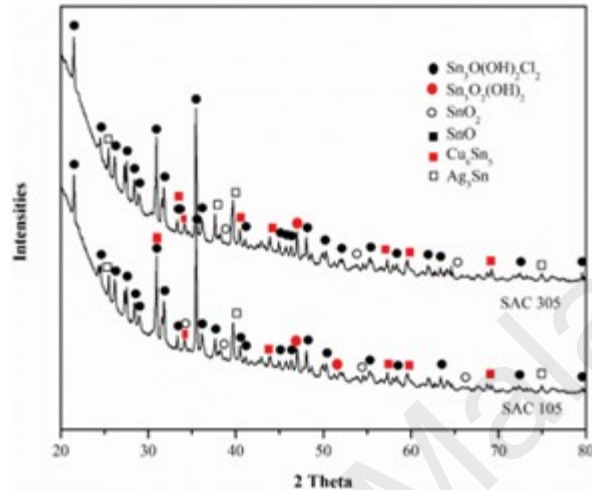


**Figure 2. 7:** X-ray diffraction scans after polarization tests for SAC305 and SAC 105 (Fayeka et al., 2017)

## 2.6 Phase diagrams for Sn-Ag-Cu (SAC) solder alloys

Initial selection of replacement solders not only depends on the cost, but they are also depends on the phase equilibrium of solder alloys system which related to the understanding of solder spreading and wetting. Much information can be obtained from phase diagram such as liquidus and solidus temperatures and also the possible formation of intermetallic phase (Suganuma, 2001).

Sn-Ag alloy system is quite important because it is commonly recognized as the most popular choice for the replacement of lead solder (Massalski et al., 1990), and the eutectic composition and temperature are Sn-3.5wt%Ag and 221°C. Additional of Cu metal as an alloying element into Sn-Ag alloy not only can improve the mechanical properties of the solder but also enhance the corrosion resistance (El-Daly et al., 2013). Since the ternary Sn-



+  $\text{Cu}_6\text{Sn}_5$ , monovariant  $\text{Ag}_3\text{Sn} + \beta\text{-Sn}$ , monovariant  $\text{Cu}_6\text{Sn}_5 + \beta\text{-Sn}$ , and eutectic  $\text{Ag}_3\text{Sn} + \text{Cu}_6\text{Sn}_5 + \beta\text{-Sn}$  (Swenson, 2007).

## 2.7 Microstructure of different alloys

Microstructure can be defined generally as the structure of a material as determined by any of the available microscopic techniques, including reflected light metallography, thin sections, electron microprobe analysis (EPMA), scanning electron microscope (SEM), scanning/transmission electron (STEM), transmission electron microscopy (TEM) and others. The microstructure of a material can strongly influence physical properties such as corrosion resistance and wear resistance. Corrosion resistance of the lead-free solder alloys can be determined through the formation of corrosion product on the surface of corroded solder alloys. Hundreds of Pb-free solder alloys have been developed due to the efforts of many researchers.

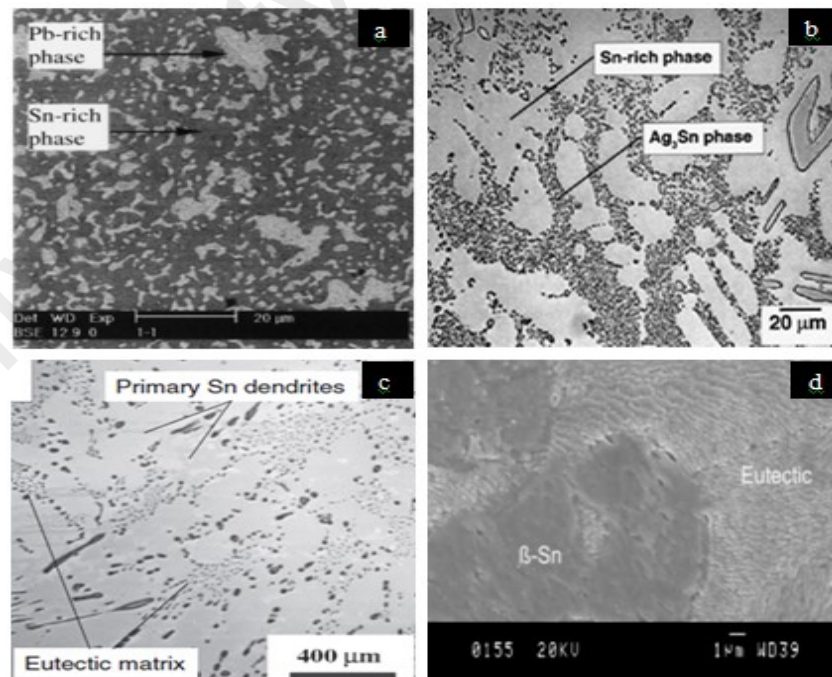


**Figure 2. 9:** SEM micrographs of different binary solder alloys: (a) Sn-Pb (Wu et al., 2006), (b) Sn-Ag (Glazer, 1994), (c) Sn-Cu (Madeni et al., 2003) and (d) Sn-Zn (Wu et al., 2004)

Sn-Pb solder alloys have a eutectic composition of Sn-37Pb and eutectic temperature of 183°C. A Sn-Pb alloy studied by Wu et al. (2006) consists of Pb-rich phases in white and Sn-rich phase in black coexist evenly (Fig. 2.9a). The eutectic Sn-3.5Ag alloy has a melting temperature of 221°C. The microstructure (Fig. 2.9b) of this system consists of a primary  $\beta$ -Sn phase and an  $\text{Ag}_3\text{Sn}$  intermetallic compound is in the form of thin platelets where its size and shape can be affected by the cooling rate (Glazer, 1994; Wu et al., 2011). Fine dispersion of  $\text{Ag}_3\text{Sn}$  was formed when the cooling rate is increased, whilst a decreased cooling rate results in needle-like  $\text{Ag}_3\text{Sn}$  (Glazer, 1994; Wu et al., 2011). The binary alloy of Sn-Cu has a eutectic composition of Sn-0.7Cu and a eutectic temperature of 227°C. The microstructure (Fig. 2.9c) of the Sn-Cu alloy is similar to that of Sn-Ag with a more elongated  $\text{Cu}_6\text{Sn}_5$  IMC (Wu et al., 2002) and dominated by primary  $\beta$ -Sn dendrites. On a Cu substrate, the solder forms with large Sn-rich dendrites interspersed with fine  $\text{Cu}_6\text{Sn}_5$  intermetallics. A thin layer of  $\text{Cu}_3\text{Sn}$  forms at the interface with a Cu substrate and a thick scallop layer of  $\text{Cu}_6\text{Sn}_5$  on top of  $\text{Cu}_3\text{Sn}$ . Sn-9Zn alloy is one of the best alternatives to Sn-Pb with a melting temperature of 199°C, as compared with 183°C of Sn-Pb. Microstructure of Sn-Zn (Fig. 2.9d) consists of two phases: a body centered tetragonal Sn matrix phase and a secondary phase of hexagonal Zn (Wu et al., 2006).

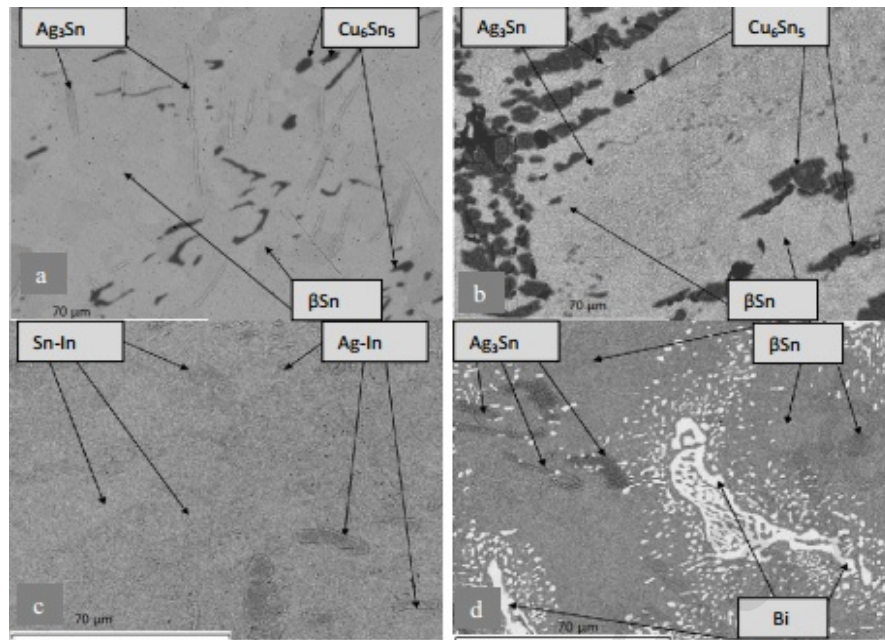


**Figure 2. 10:** SEM micrographs of different ternary solder alloys: (a) Sn–3.1Ag–0.8Cu, (b) Sn–2.9Ag–6.7Cu, (c) Sn–2.3Ag–9In and (d) Sn–3.0Ag–10.4Bi (Rosalbino et al., 2008)

As for ternary system, Sn-Ag-Cu alloys were considered as the best replacement for Pb-free solder. Rosalbino et al. (2008) had studied the corrosion behavior assessment of ternary system of Sn-Ag solder with addition of different alloying element such as In, Bi and Cu. The results showed that the microstructure of the Sn–3.1Ag–0.8Cu alloy (Fig. 2.10a) consists a typical three-phase appearance with a matrix of  $\beta$ Sn where  $\text{Cu}_6\text{Sn}_5$  (black crystals) and  $\text{Ag}_3\text{Sn}$  (grey crystals with needle shape) are dispersed. The observed solubility of Ag in the  $\eta$  phase and of Cu in the  $\epsilon$  phase is very small, likewise for the Cu and Ag solubility in Sn. Meanwhile, the microstructure of the Sn–2.9Ag–6.7Cu alloy (Fig. 2.10b) consist the matrix of  $\beta$ Sn where many  $\text{Cu}_6\text{Sn}_5$  (large black crystals) are precipitated and a few  $\text{Ag}_3\text{Sn}$  particles very finely dispersed in the matrix. The microstructure of Sn–2.3Ag–9In alloy (Fig. 2.10c) consists almost completely of  $\gamma$  (Sn–In) phase where very few crystals of  $\zeta$  (Ag–In) phase are dispersed. The microstructure of Sn–3.0Ag–10.4Bi alloy (Fig. 2.10d) shows the coexistence of three phases consisting of  $\text{Ag}_3\text{Sn}$  (grey crystals) and

large white crystals of Bi dispersed in the  $\beta$ Sn matrix. Table 2.8 shows the eutectic temperature and eutectic composition of the binary and ternary solder alloys which are mostly used in the electronic industry nowadays.

**Table 2. 8:** Eutectic temperature and composition of the solder alloys

System	Eutectic temperature (°C)	Eutectic composition (wt- %)	Reference
Sn-Pb	183	Sn-37Pb	(King, 1988)
Sn-Cu	227	Sn-0.7Cu	(Bilek et al., 2006)
Sn-Ag	221	Sn-3.5Ag	(King, 1988)
Sn-Au	217	Sn-10Au	
Sn-Zn	199	Sn-9Zn	(Zeng & Tu, 2002)
Sn-In	120	Sn-51In	
Sn-Bi	139	Sn-57Bi	
Sn-Ag-Bi	208-217	Sn-3.5Ag-3Bi	(Smith et al., 2002)
Sn-Zn-Bi	192-197	Sn-8Zn-3Bi	
Sn-Ag-Cu	217	Sn-3.8Ag-0.7Cu	(Bilek et al., 2006)
	218	Sn-3.5Ag-0.5Cu	(Smith et al., 2002)

## 2.8 Summary and conclusions

From the literature study done so far, the following conclusions could be drawn:

- i. Physical, mechanical, thermal and electrical properties are the important key to analyzed solder properties. A good lead-free solder alloys must have closet properties to the conventional Sn-Pb alloys.
- ii. The addition of alloying elements such as Ag, Cu, Zn, Bi, In, etc. would affect the characteristics of the solder alloys including corrosion resistance. Sn, Ag and Cu

added solder alloys had better corrosion resistance while the addition of Zn lower the corrosion resistance of the solders.

- iii. As a good alternative alloys, lead-free solder alloys must affordable. All of the Pb-free solder alloys are more expensive than the eutectic Pb-Sn alloy and Indium is the most expensive alloy as compared to others.
- iv. Through the SEM images, the corrosion products and intermetallics compounds form on the surface of binary solders (Sn-Ag, Sn-Cu, Sn-Zn and Sn-Pb) and ternary solders (Sn-Ag-Cu, Sn-Ag-Bi and Sn-Ag-In) were  $\beta$ Sn,  $\text{Ag}_3\text{Sn}$ ,  $\text{Cu}_6\text{Sn}_5$  and mostly was tin oxychloride (grey phase).
- v. Due to the lower passivation range, lead-free solder exhibits better corrosion resistance than Sn-Pb solder.

## CHAPTER 3: RESEARCH METHODOLOGY

### 3.1 Introduction

This chapter describes the detailed steps involved in the samples' preparation and corrosion test characterization. There are 3 stages to conduct the experiments for this project. These are: (a) Metal sample and solution preparation for the electrochemical corrosion tests, (b) Corrosion tests by Potentiodynamic Polarization, Electrochemical Impedance Spectroscopy (EIS) and (c) Metal surface characterization of the lead free solder alloys before and after the corrosion test. Fig. 3.1 shows the flowchart for experimental works. The materials and apparatus used in the present research are listed below.

- a) Lead-free solder alloys:
  - i) Sn-1.0Ag-0.5Cu
  - ii) Sn-1.0Ag-0.5Cu-0.1Zn
  - iii) Sn-1.0Ag-0.5Cu-0.5Zn
  - iv) Sn-1.0Ag-0.5Cu-1.0Zn
  - v) Sn-1.0Ag-0.5Cu-0.1Al
  - vi) Sn-1.0Ag-0.5Cu-0.5Al
  - vii) Sn-1.0Ag-0.5Cu-1.0Al
- b) Acetone
- c) Sodium chloride powder
- d) Drilling machine and threading die set
- e) Weighing machine
- f) Polishing machine and Silicon carbide paper
- g) Potentiostat (Gamry Echem Analyst DC105 software)

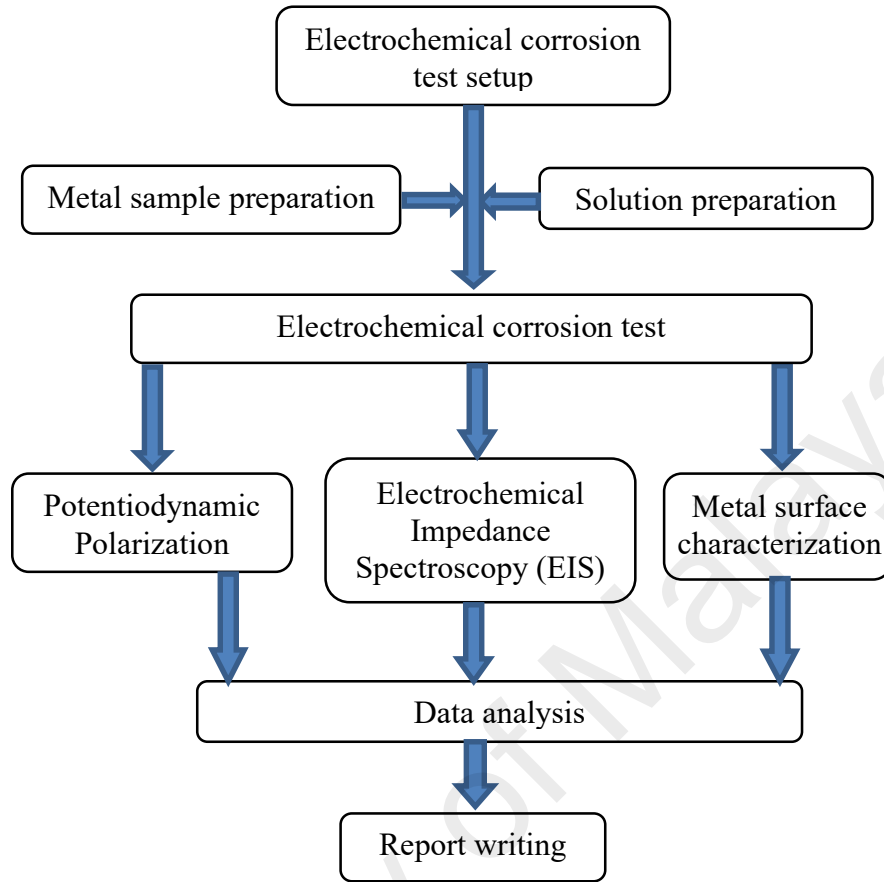


**Figure 3. 1:** Flowchart of experimental works

### 3.2 Sample and solution preparation

Commercially available Sn-1.0Ag-0.5Cu, Sn-1.0Ag-0.5Cu-0.1Zn, Sn-1.0Ag-0.5Cu-0.5Zn, Sn-1.0Ag-0.5Cu-1.0Zn, Sn-1.0Ag-0.5Cu-0.1Al, Sn-1.0Ag-0.5Cu-0.5Al and Sn-1.0Ag-0.5Cu-1.0Al solder bars were cut into block with exposed surface area  $\pm 1\text{cm}^2$  (Fig. 3.2). A blind hole with a 1.6 mm diameter was drilled on the blocks surface. Prior to the test, the sample surfaces were first polished with SiC papers of grit 800, 1000, 1200 and 1500. The sample then cleaned with acetone and distilled water to remove impurities.

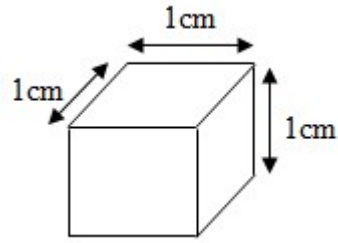


**Figure 3. 2:** Sample dimension

For corrosion test, a solution of 3.5wt-% NaCl was used. In order to obtain 3.5wt-% of NaCl solution, 35g NaCl powder was mixed into 1000ml of distilled water as per following calculation. The solution was stirred by using magnetic stirrer bar for 10 minutes.

$$\text{Weight \%} = \frac{\text{mass of solute (g)}}{\text{volume of solution}} \times 100\%$$

$$3.5 = \frac{\text{mass of solute}}{1000} \times 100\%$$

$$\text{Mass of solute} = 10 \times 3.5 = 35\text{g}$$

### 3.3 Corrosion test

Potentiodynamic polarization test and electrochemical impedance spectroscopy (EIS) test were used to determine the corrosion behavior of the SAC 105 solder alloy. The whole experiment was divided into two sets of test. Fig. 3.3 shows the chart for set 1-2. For experimental set 1, the corrosion behavior of Sn-1.0Ag-0.5Cu-*X*Zn (*X*= 0, 0.1, 0.5, 1.0) in terms of potentiodynamic polarization test and EIS was investigated while set 2 deals the similar things for Sn-1.0Ag-0.5Cu-*X*Al (*X*=0, 0.1, 0.5, 1.0).

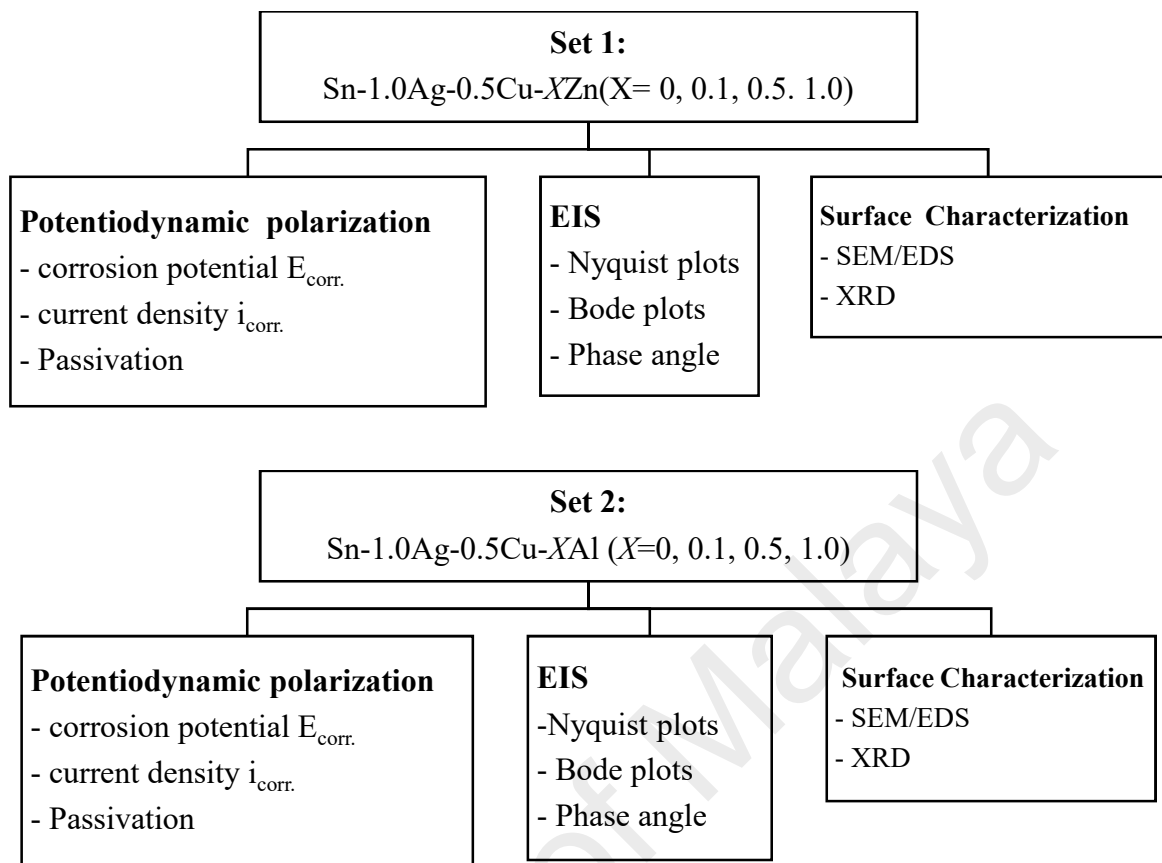


**Figure 3. 3:** Experimental design for set 1 to set 2

### 3.3.1 Electrochemical test setup

The test cell was conducted in the standard three-electrode cell consisted of (a) solder material with  $\pm 1\text{cm}^2$  of exposed area as a working electrode (WE), (b) platinum foil as a counter electrode (CE) and (c) silver-silver chloride electrode as reference electrode (RE) with a Luggin capillary bridge connected to the test solution (Fig. 3.4). Before running the corrosion test, the calibration test was completed so that more accurate results could be obtained.

The corrosion test could be started right after the calibration test. Three of the test cells were recommended to be placed as near as possible but not touching each other to obtain better and accurate results. Besides that, the distance among three of the test cells must be

same for every test. All experiments were carried out at room temperature (25-27°C) and the surface observed to be corroded after the corrosion tests.

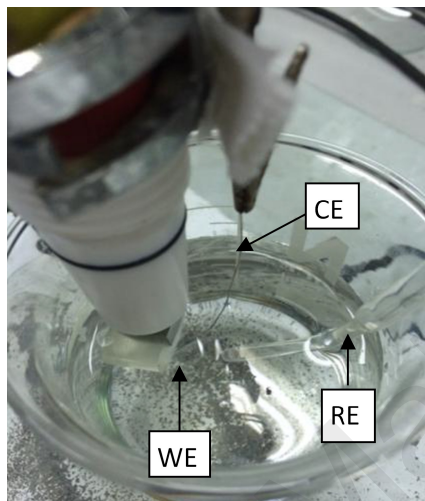


**Figure 3. 4:** Electrochemical setup.

### **3.3.2 Potentiodynamic Polarization**

The initial and final potential defined the ‘path’ which the scan will take place. Meanwhile the scan rate refers to the rate which the potential was varied when the potentiodynamic scan was running. In this potentiodynamic polarization test, the initial potential was set at -1V and final potential at +1V vs. SCE reference electrode at a scan rate of 1mV/s.

### **3.3.3 Electrochemical Impedance Spectroscopy (EIS)**

Electrochemical impedance spectroscopy (EIS) was measured at the open circuit potential using a Gamry G300 Potentiostat/Galvanostat (Gamry Instruments, Inc., USA). The frequency range analyzed was 100 kHz to 0.01Hz, with the frequency values spaced logarithmically (ten per decade). Nyquist plot for all samples were plotted in a same graph

to make a comparison of polarization resistance ( $R_p$ ).  $R_p$  is obtained from the diameter of the semicircle.

### **3.4 Surface characterization**

Before and after the electrochemical corrosion test, the sample surfaces were characterized by scanning electron microscopy (SEM) equipped with energy-dispersive X-ray spectroscopy (EDS) analysis and X-ray Diffraction (XRD).

University of Malaya

## CHAPTER 4: RESULTS AND DISCUSSION

### 4.1 Introduction

This chapter present the results obtained from different experiment and were divided into 2 set which were distinguished by the materials used; Set 1: Corrosion behavior of Zn-containing solder alloys in 3.5wt-% NaCl solution and Set 2: Corrosion behavior of Al-containing solder alloys in 3.5wt-% NaCl solution.

### 4.2 Corrosion behavior of Zn-containing solder alloys in 3.5wt-% NaCl solution

This chapter present the results obtained from different experiment to evaluate the effect of Zinc concentration on the corrosion behavior of SAC105 solder alloy.

#### 4.2.1 Potentiodynamic polarization curves

Fig. 4.1 shows the potentiodynamic polarization curves for SAC105, SAC105+0.1Zn, SAC105+0.5Zn and SAC105+1.0Zn solder alloys in 3.5wt-% NaCl solution. It is seen that the shape of the polarization curves exhibit a typical active-passive-transpassive behaviour associated with the formation of passive films.

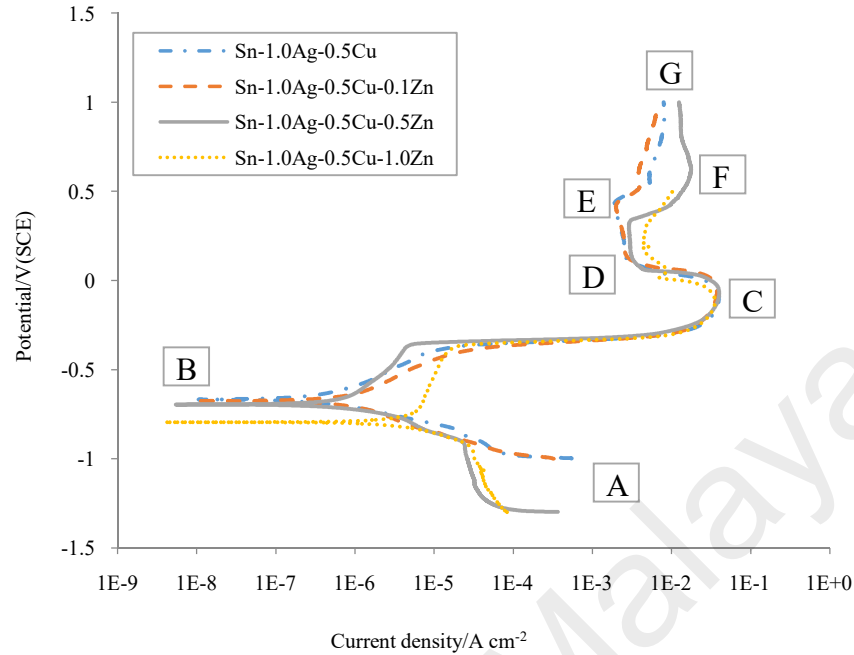
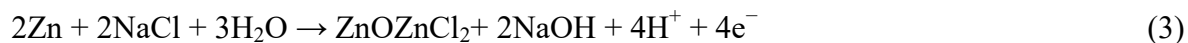


**Figure 4. 1:** Potentiodynamic polarization curves of SAC105, SAC105+0.1Zn, SAC105+0.5Zn and SAC105+1.0Zn solder alloys in 3.5wt-% NaCl solution

Region AB in the Fig. 4.1 denotes cathodic activation process. Since all corrosion tests were performed in NaCl solution, the cathodic branch of polarization curves could be ascribed to the dissolved oxygen reduction in water resulting in the formation of hydroxyl ion according to the following reaction (1) (Ahmido et al., 2011):



The corrosion potential  $E_{corr.}$ , where the extrapolated anodic and cathodic Tafel slopes intersect and the current becomes zero was denoted at point B. In the anodic direction, increasing potential up to  $E_{corr.}$  may induce the zinc dissolution according to the following reactions (2-3):



Region BC in the Fig. 4.1 denotes anodic activation reaction and there is a sharp increase in current density which might be attributed to the active dissolution of Sn and Sn(II) species according to the reactions (4-5) below:



With increasing the potential, the active dissolution of zinc continues until the zincate concentration reaches a maximum value and supersaturated the surface of the solder. The surface of the corroded samples was covered by the insoluble zincate and created a plateau region (DE) where the current density was found to be independent of potential over approximate range of 500 mV. Then the curve runs into transpassive region EF as shown in the Fig. 4.1 where the current density begins to rise at high potential due to the breakdown of the passive oxide layer and formation of pits (Wu et al., 2006). At point G, the formation of the corrosion product again covers the surface of the solder avoiding further corrosion.

The electrochemical data extracted from these curves are summarized in Table 4.1. It is seen that the SAC105 solder alloy exhibits a corrosion potential ( $E_{corr.}$ ) of -668 mV(SCE). With the addition of 0.1wt-% Zn, corrosion potential slightly decreases to -676 mV(SCE).  $E_{corr.}$  values are decreased to -696 and -795 mV(SCE) with the addition of 0.5 and 1.0-wt%

Zn respectively. SAC105+1.0Zn exhibit the lowest  $E_{corr.}$  value which could be attributed to the formation of Zn-rich phase in the Sn-matrix (Chang et al., 2006).

**Table 4. 1:** Potentiodynamic polarization parameters for SAC105, SAC105+0.1Zn, SAC105+0.5Zn and SAC105+1.0Zn solder alloys in 3.5wt-% NaCl solution

Materials	$E_{corr.}$ (mV)	$I_{corr.}$ (mA/cm <sup>2</sup> )	$I_{cc}$ (mA/cm <sup>2</sup> )	$I_{pass.}$ (mA/cm <sup>2</sup> )	$E_{pass.}$ (mV)	$\Delta E$ (mV)	Corrosion rate (mpy)
SAC105	-668	$0.451 \times 10^{-3}$	36.0	2.56	-168.0	285.3	0.07
SAC105+0.1Zn	-676	$0.705 \times 10^{-3}$	35.7	2.57	-117.5	274.3	0.09
SAC105+0.5Zn	-696	$0.891 \times 10^{-3}$	37.2	3.38	-129.3	231.0	0.12
SAC105+1.0Zn	-795	$9.720 \times 10^{-3}$	35.2	4.69	-130.4	158.6	1.25

The corrosion current density  $I_{corr.}$ , represents the corrosion rate of the system. The corrosion current density is the lowest ( $0.451 \times 10^{-3}$  mA/cm<sup>2</sup>) for SAC105 alloy. With the addition of 0.1 and 0.5wt-% Zn content in the alloy,  $I_{corr.}$  were increased to  $0.705 \times 10^{-3}$  mA/cm<sup>2</sup> and  $0.891 \times 10^{-3}$  mA/cm<sup>2</sup> respectively. SAC105+1.0Zn alloy having the highest corrosion current density ( $9.72 \times 10^{-3}$  mA/cm<sup>2</sup>) demonstrates the worst corrosion resistance. We can conclude that  $I_{corr.}$  increase with Zn content. SAC105 is more resistant to corrosion as compared to Zn-containing solder alloys. These results were in accordance with the study conducted by other researchers (Wu et al., 2004). Wu et al., (2004) studied the electrochemical corrosion of Pb-free solders alloy and they found that Zn-containing alloys (Sn-9Zn and Sn-8Zn-3Bi) have the worst corrosion behaviour in acid solutions as compared to Sn-3.5Ag-0.5Cu solder alloy.

The current density and potential at point C in the Fig. 4.1 are known as critical current density  $I_{cc}$  and passivation potential  $E_{pass.}$ . SAC105 exhibits  $I_{cc}$  value, 36 mA/cm<sup>2</sup>, which slightly decreased upon addition of 0.1wt-% Zn exhibiting  $I_{cc}$  value of 35.7 mA/cm<sup>2</sup>.  $I_{cc}$

kept decreasing to  $35.2 \text{ mA/cm}^2$  when the Zn content was 1.0wt-% as shown in Table 4.1. The current density at the passive range of DE in the Fig. 4.1 is known as passive current density  $I_{pass.}$ . The value of  $I_{pass.}$  for SAC105 is  $2.56 \text{ mA/cm}^2$  which increases to  $2.57 \text{ mA/cm}^2$  with 0.1wt-% Zn additions. It is seen that the  $I_{pass.}$  values for SAC105 keeps on increasing to  $4.69 \text{ mA/cm}^2$  when the Zn content increased to 1.0wt-%. Larger passivation range and lower passivation current density indicates higher corrosion resistance and more stable protective passive film on the surface.

From Fig. 4.1, it is seen that SAC105 and SAC105+0.1Zn solder alloys have almost same passivation range. SAC105+1.0Zn have smallest (158.6 mV) passivation range. This indicates that SAC105+1.0Zn have lowest corrosion resistance as compared to other alloys which could be attributed to the increase of the Zn content. SAC105 exhibits better corrosion resistance due to the largest passivation range and the lowest passivation current density (Li et al., 2008; Rosalbino et al., 2009).

Overall view from Fig. 4.1 shows breakdown that occurs early for SAC105+1.0Zn as compared to other solder alloys. Addition of Zn shifted the corrosion current density and passivation current density towards more positive values. This suggested that Zn reduced corrosion resistance. Due to the higher corrosion potential, lower passivation current density and corrosion current density, the corrosion resistance of SAC105 solder alloy is somewhat better than other solder alloys.

#### **4.2.2 Corrosion rate**

The corrosion rate was obtained by Tafel fit using Gamry Echem Analyst DC105 software and the data was listed in Table 4.1 for Zn-containing solder. From Table 4.1, it is seen that SAC105 solder alloy shows the lowest corrosion rate, 0.07 mpy. When 0.1wt-% of Zn was added, the corrosion rate was increased to 0.09 mpy. Corrosion rate of SAC105 solder alloy kept increasing to 0.12 mpy when 0.5wt-% of Zn was added. For the addition of 1.0wt-% of Zn was added, the corrosion rate increased to the highest value (1.25 mpy) among all the alloys tested. As a result, it can be concluded that SAC105+1.0Zn solder alloy deteriorates and corrodes more rapidly with the low corrosion resistance and highest corrosion rate.

#### **4.2.3 Morphological, elemental and phases analyses of corrosion products**

In Fig. 4.2, the SEM micrographs reveal the morphology of SAC105, SAC105+0.1Zn, SAC105+0.5Zn and SAC105+1.0Zn solder alloys at as-received condition and alloys surface at the end of the potentiodynamic polarization tests. The structure of the as-received solder alloys (Fig. 4.2a-4.2d) was totally different compared with tested alloys. Most surfaces of the tested samples were covered by corrosion product, as shown in Fig. 4.2e-4.2h.

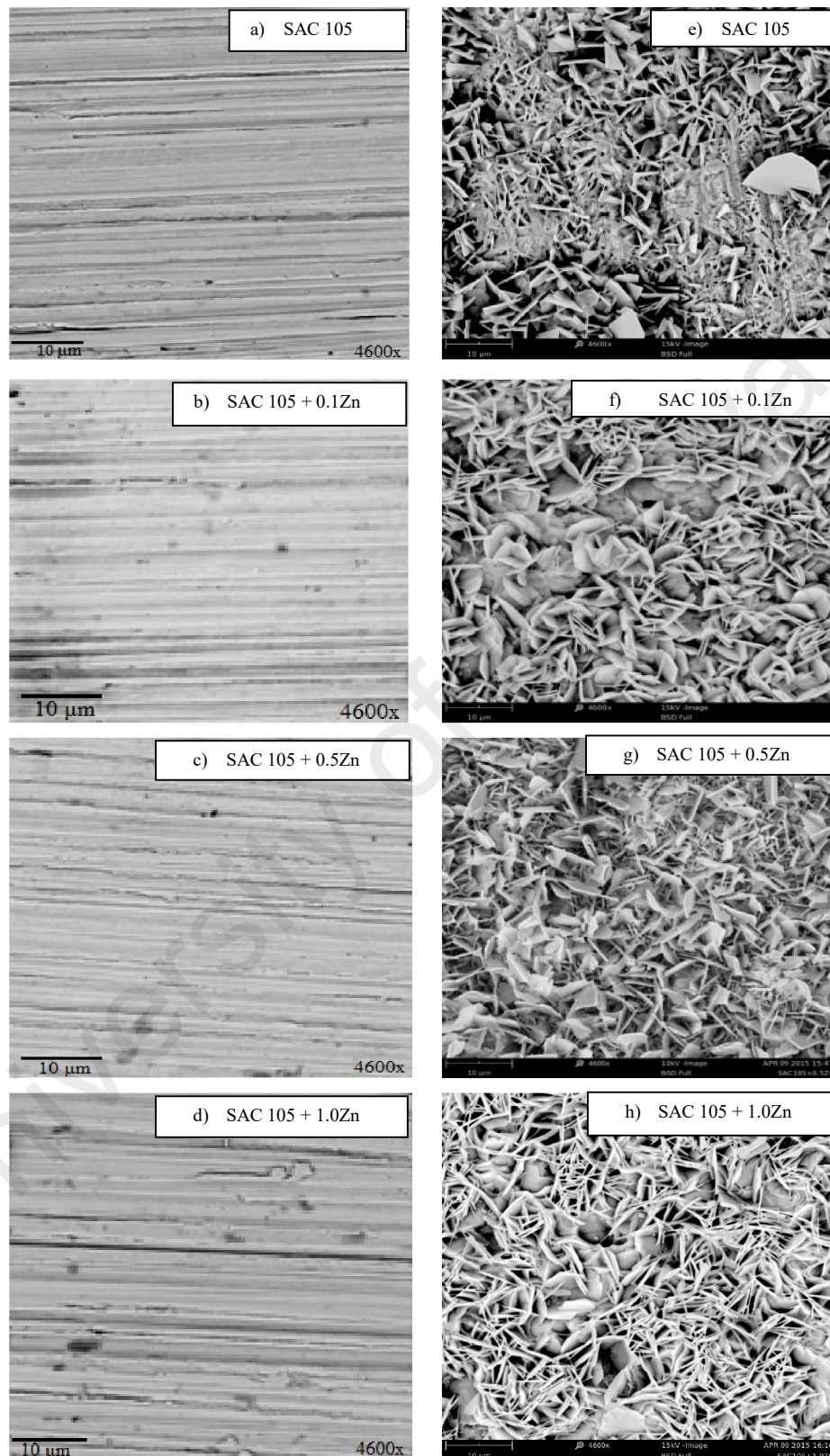


**Figure 4. 2:** SEM micrographs (4600x) of SAC105, SAC105+0.1Zn, SAC105+0.5Zn and SAC105+1.0Zn solder alloys before (a-d) and after (e-h) the corrosion test

**Table 4. 2:** Mass percentage of elements present in different alloy surfaces after potentiodynamic polarization test

Mass percentage	Sn	Cl	O	Zn
SAC105	19.3	18.5	60.8	-
SAC105+0.1Zn	14.7	12.3	64.7	0.3
SAC105+0.5Zn	24.1	16.8	41.4	0.4
SAC105+1.0Zn	26.7	24.5	47.1	0.8

The corrosion products formed on coupons after potentiodynamic polarization tests had only a platelet-like shape and were loosely distributed on the surface with different orientations (Fig. 4.2e). Table 4.2 shows the surface element concentrations of sample corrosion products as determined by EDS. According to the EDS analysis, the corrosion products of SAC105 solder alloy contained mainly Sn, Cl and O, at 19.3wt-%, 18.5wt-%, and 60.8wt-%, respectively. Percentage of Cl and Zn were found to be increased with the increase of Zn content in solder alloys. This suggested that Cl may have greater influence on the formation of Zn-based corrosion products. The corrosion products formed on the coupon are found to be larger in size when Zn content was added into SAC105 (Fig. 4.2f-4.2h).

The differences in corrosion resistance can be explained by the formation of a more compact corrosion product film. The corrosion products will block the access of the electrochemically active species to electrode surface, limiting the ion diffusion to the surface and thus reducing the overall corrosion reaction rate (Gabrielli & Group, 1980). Hereby, ion diffusion is referring to the movements of electrochemically active species from a region of high concentration to a region of low concentration. Therefore, based on the Fig. 4.2e-4.2h, the corrosion resistance of SAC105 solder alloy is higher than Zn-containing solder alloy.

The EDS analysis reveals the increase in quantity of Zn on the surface (Table 4.2). It is noted that the presence of  $\text{Cl}^-$  on the surface and the quantity of this ion increase with Zn content. Film was mechanically breakdown due to the penetration of chloride ion into the oxide film and form metal chloride (Pistorius & Burstein, 1994). Halide ions also stimulate the active dissolution of zinc and result in breakdown of the passive film as reported by other researchers (Assaf et al., 1999).

Fig. 4.3 shows the XRD patterns after polarization for SAC105, SAC105+0.1Zn, SAC105+0.5Zn and SAC105+1.0Zn solder alloys in 3.5wt-% NaCl solution. The XRD patterns reveal the presence of  $\text{Sn}_3\text{O}(\text{OH})_2\text{Cl}_2$  (ICDD 00-039-0314), SnO (ICDD 98-002-0624) and  $\text{SnO}_2$  (ICDD 98-003-9178) on the exposed surface of solder. Addition of ZnO (ICDD 98-006-7454) was detected on Zn-containing solder alloys. When the potentials move to a further anodic direction, it is believed that the ZnO tends to dissolved (Lin & Liu, 1998a). Therefore, the products formed at the surface area are almost due to the oxidation of zinc (Ahmido et al., 2011).

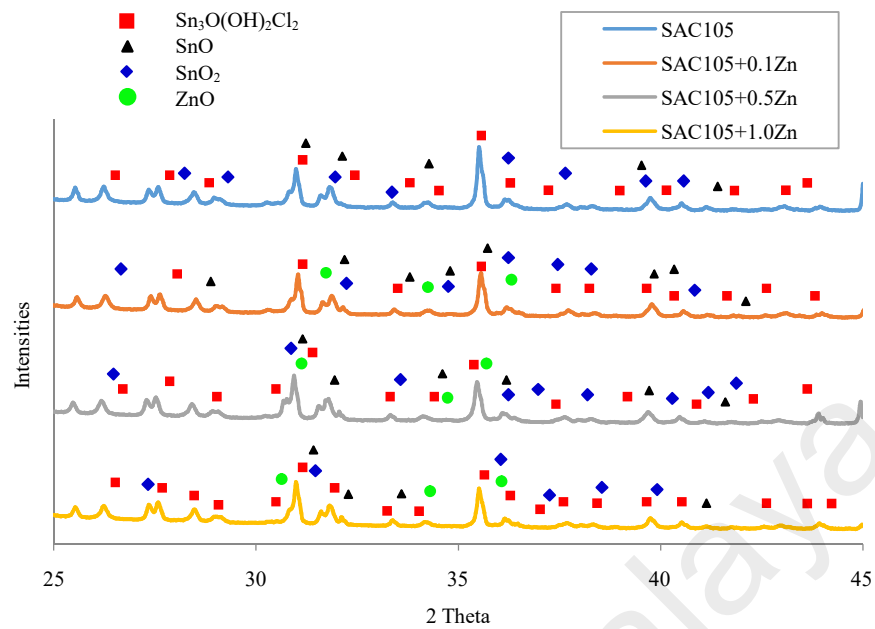


**Figure 4. 3:** X-ray diffraction scans after polarization for SAC105, SAC105+0.1Zn, SAC105+0.5Zn and SAC105+1.0Zn solder alloys in 3.5wt-% NaCl solution

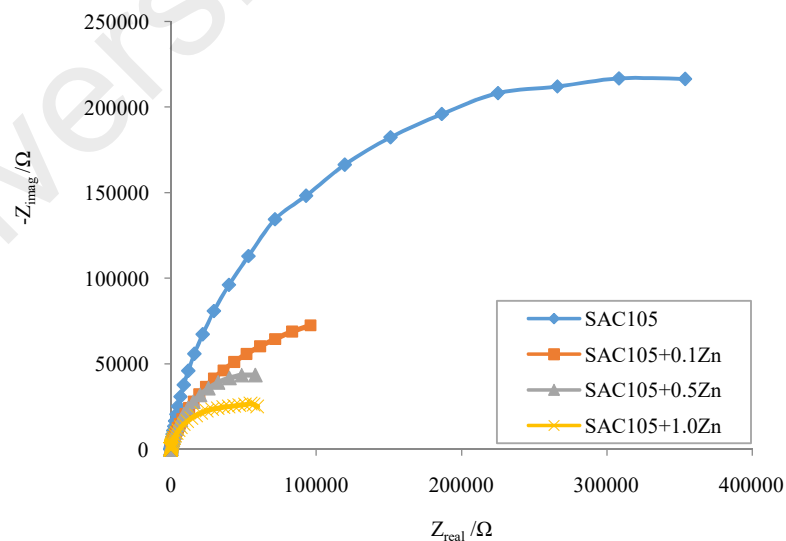
From the XRD analysis in Fig. 4.3, it can be seen that surface of the solder alloys are covered by the main product tin oxychloride ( $\text{Sn}_3\text{O}(\text{OH})_2\text{Cl}_2$ ). This result was in accordance with the previous study conducted by other researchers (Li et al., 2008; Rosalbino et al., 2008). Rosalbino et al. (2008) studied the potentiodynamic polarization of Sn-Ag-Cu solders in aerated 0.1M NaCl reported that corrosion products constituted by tin oxychloride are present at the corroded surface after the test. The formation of a tin oxychloride layer according to the following reaction (6) (Ervina & Amares, 2014):



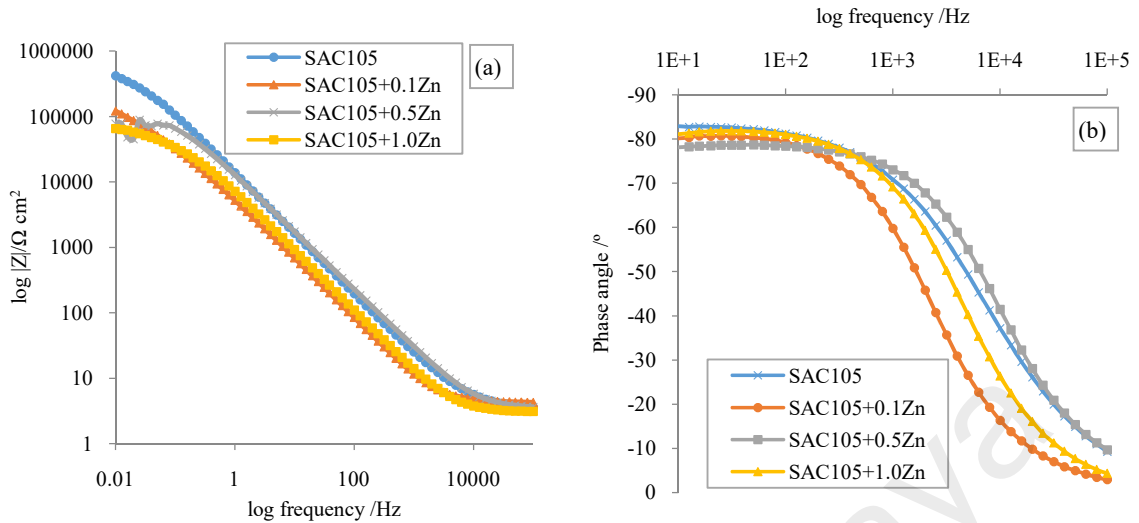
#### 4.2.4 Electrochemical Impedance Spectroscopy (EIS)

Fig. 4.4 and Fig. 4.5 illustrated the electrochemical impedance spectra of different solder alloys. Nyquist plots are characterized by a semicircle or capacitive loop from high to low frequency where these capacitive loops are ascribed to the double layer capacitance and charge transfer resistance. The diameter of Nyquist semicircle corresponds to the polarization resistance ( $R_p$ ) and it increases as the corrosion resistance increases (Bobina et al., 2013). It is important to remark that the highest capacitive arc induces the best electrochemical corrosion resistance.

It is seen in Fig. 4.4 that all solder alloys exhibits a nearly straight diagonal line throughout the whole frequency region correspond to diffusion-induced Warburg-like impedance. The loop diameter decreases with the addition of Zn. This demonstrates that Zn-doped solder alloys undergo more corrosion (Lee et al., 2008).



**Figure 4. 4:** Nyquist plot for SAC105, SAC105+0.1Zn, SAC105+0.5Zn and SAC105+1.0Zn solder alloys in 3.5wt-% NaCl solution



**Figure 4. 5:** Bode plots (a) Magnitude Bode plot and (b) Phase Angle Bode plot for SAC105, SAC105+0.1Zn, SAC105+0.5Zn and SAC105+1.0Zn solder alloys in 3.5wt-% NaCl solution

Fig. 4.5 depicts the Bode plot and Bode-phase angle plot representing the modulus of impedance and phase angle as a function of frequency for different solder alloys. The impedance magnitudes of the four solder alloy samples at lowest frequency have been listed in Table 4.3. The magnitude of impedance  $|Z|$  and maximum phase angle  $\theta_{max}$  can be used to determine the corrosion resistance of solder alloys. Higher magnitude of impedance (Fig. 4.5a) and higher maximum phase angle (Fig. 4.5b) represent better corrosion resistance.

**Table 4. 3:** Electrochemical impedance spectroscopy parameters for SAC105, SAC105+0.1Zn, SAC105+0.5Zn and SAC105+1.0Zn solder alloys in 3.5wt-% NaCl solution

Solder alloys	Log $ Z /\Omega \text{ cm}^2$	$\theta_{max}/^\circ$
SAC105	414 800	-82.67
SAC105+0.1Zn	120 200	-80.67
SAC105+0.5Zn	77 490	-78.63
SAC105+1.0Zn	64 600	-81.80

It is known that the Bode plot provides the maximum magnitude of impedance ( $|Z|$ ) at low frequencies (Fig. 4.5a). In this context, at a frequency of 0.01 Hz, the highest magnitude of impedance,  $414\ 800\ \Omega\ \text{cm}^2$ , can be observed for the SAC105 indicating the highest corrosion resistance which is attributed to the formation of comparatively more adherent and protective oxide film on the surface. On the other hand, SAC105 solder alloy also exhibit the largest maximum phase angle ( $\theta_{max}$ ),  $-82.67^\circ$  which confirms its highest corrosion resistance.

For SAC105+0.1Zn solder alloy, the values of impedance and maximum phase angle are  $120\ 200\ \Omega\ \text{cm}^2$  and  $-80.67^\circ$  respectively. When concentration of Zn increased to 0.5wt-%, both impedance and maximum phase angle decreased to  $77\ 490\ \Omega\ \text{cm}^2$  and  $-78.63^\circ$  respectively. With 1.0wt-% Zn, impedance and maximum phase angle has lowest value. It can be concluded that SAC105 solder alloy exhibits better corrosion resistance as compared to others. This could be attributed to reduced active surface due to the formation of corrosion product layer that act as an effective barrier against further corrosion.

### **4.3 Corrosion behavior of Al-containing solder alloys in 3.5wt-% NaCl solution**

This chapter presents the results obtained from different tests to evaluate the effect of Aluminium concentration on the corrosion behavior of SAC105 solder alloy.

#### **4.3.1 Potentiodynamic polarization curves**

The potential-current density profiles plot of the Sn-Ag-Cu- $X$ Al ( $X=0, 0.1, 0.5, 1.0$ ) solders generated by the potentiodynamic polarization studies carried out in 3.5wt-% NaCl solution are reported in Fig. 4.6. Since all corrosion tests were performed in aerated NaCl solution

the cathodic branch of polarization curves may be ascribed to the dissolved oxygen reduction reaction (7):

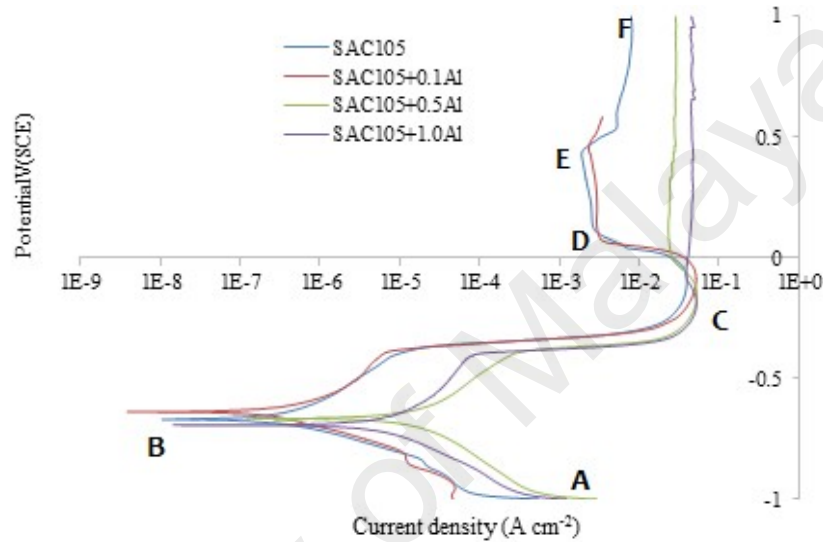


**Figure 4. 6:** Potentiodynamic polarization curves of SAC105, SAC105+0.1Al, SAC105+0.5Al and SAC105+1.0Al solder alloys in 3.5wt-% NaCl solution

The anodic excursion of the potential scan starts at point B which is referred to as  $E_{corr}$ . (corrosion potential), where the extrapolated anodic and cathodic Tafel slopes intersect and the current becomes zero. Increasing the potential up to  $E_{corr}$ . may induce the dissolution of Al. The anodic reactions (8-10) for dissolution of Al can occur by the following steps (Mohanty & Lin, 2006a):



The active dissolution of Al can be explained by the potential difference existing among the alloy. Table 4.4 shows that the electrode potential of Ag, Cu and Sn are much higher compared with that of Al. Thus, Al was considered as the most active among these metals. As a result, Al acts as an anode in the alloy and, therefore, more easily dissolves in corrosive conditions.

**Table 4. 4:** Electrode potential of solder elements

Element	Reaction	Electrode potential (V)
Silver	$\text{Ag}^{2+} + \text{e}^- = \text{Ag}$	+ 0.7996
Copper	$\text{Cu}^+ + \text{e}^- = \text{Cu}$	+0.5210
	$\text{Cu}^{2+} + 2\text{e}^- = \text{Cu}$	+0.3419
Tin	$\text{Sn}^{2+} + 2\text{e}^- = \text{Sn}$	-0.1375
Aluminium	$\text{Al}^{3+} + 3\text{e}^- = \text{Al}$	-1.6600

$\text{Al}(\text{OH})_3$  production and deposition causes Al depletion. The active dissolution of Al continues with increasing potential until the hydroxide ( $\text{OH}^-$ ) concentration reaches a critical value and supersaturates the surface of the alloy at point C. The surface of the corroded samples was covered by the insoluble hydroxide and created a plateau region (DE) where the current density was found to be independent of potential. It is noted that Al is the minor element in SAC105, Al is quickly depleted or blocked by  $\text{Al}(\text{OH})_3$  on the surface which has exposed the metal Sn underneath. Thus, as the second most active material after Al in this system, Sn can be dissolved to Sn(II) species (Drogowska et al., 1991; Stirrup & Hampson, 1977) according to the reactions (11-12) displayed below:



The electrochemical data extracted from these curves are summarized in Table 4.5. It is seen that the SAC105 solder alloy exhibits the corrosion potential of -668 mV(SCE). With the addition of 0.1wt-% Al, the corrosion potential increases to -637 mV(SCE). However, as 0.5wt-% and 1.0wt-% Al is added to the SAC105 solder alloy, the corrosion potential of the solder decreases to -669 mV(SCE) and -692 mV(SCE) respectively.

The corrosion-current density  $I_{corr}$  are dominated at the intersection of the Tafel lines which represent the corrosion rate of the system. From Fig. 4.6, it is seen that the shape of the polarization curves for SAC105 and SAC105+0.1Al solder alloy is almost similar and there is no significant difference of corrosion rate between these two alloys. The corrosion current density of SAC105 solder alloy is  $0.451 \times 10^{-3} \text{ mA/cm}^2$ , which is slightly lower than that of  $0.526 \times 10^{-3} \text{ mA/cm}^2$  for SAC105+0.1Al solder alloy. However, the addition of 0.5wt-% and 1.0wt-% Al into SAC105 solder alloy shifted the corrosion current density to more positive values indicates an increase in corrosion rate. The corrosion current density of SAC105+0.5Al and SAC105+1.0Al solder alloy is  $11.1 \times 10^{-3}$  and  $11.6 \times 10^{-3} \text{ mA/cm}^2$  respectively. Therefore, we can conclude that the addition of Al tends to decrease the corrosion resistance of the solder. These results are in accordance with that obtained by Mohanty and Lin (2006a) when they investigated the effect of Al concentration on the corrosion behaviour of Sn-Zn-Al-Ga alloy. Mohanty and Lin (2006a) reported that the corrosion current density and corrosion rate of Sn-8.5Zn-XAl-0.5Ga was increases significantly with increase in Al content.

At potential more positive than B, corrosion rate increases, and reaches a maximum at the passivation potential, C, which is often given the symbol,  $E_{pass}$ . and critical current density defined by symbol  $I_{cc}$ . At the passivation potential, the transition from active dissolution

occurs as solid species (oxide/hydroxide of Al and Sn) becomes more stable than the parent metal ion (Osorio et al., 2011). The surface of the electrode and passivation was covered by these oxide/hydroxides thus begins to set in, thereby decreasing the current density with further increase in potential to point D (Fig. 4.6). The current density observed in the passive region DE is referred to as the passivation current density ( $I_{pass.}$ ).

**Table 4. 5:** Potentiodynamic polarization parameters for SAC105, SAC105+0.1Al, SAC105+0.5Al and SAC105+1.0Al solder alloys in 3.5wt-% NaCl solution

Materials	$E_{corr.}$ (mV)	$I_{corr.}$ (mA/cm <sup>2</sup> )	$I_{cc}$ (mA/cm <sup>2</sup> )	$I_{pass.}$ (mA/cm <sup>2</sup> )	$E_{pass.}$ (mV)	$\Delta E$ (mV)	Corrosion rate (mpy)
SAC105	-668	$0.451 \times 10^{-3}$	39.8	2.55	-120.6	285.3	0.07
SAC105+0.1Al	-637	$0.526 \times 10^{-3}$	51.3	2.98	-110.8	347.6	0.08
SAC105+0.5Al	-669	$11.100 \times 10^{-3}$	52.1	24.30	-134.6	-	1.44
SAC105+1.0Al	-692	$11.600 \times 10^{-3}$	52.0	38.80	-158.5	-	1.49

From Table 4.5, it is seen that SAC105 solder exhibits smallest  $I_{cc}$  (39.8 mA/cm<sup>2</sup>) and  $I_{pass}$  (2.55 mA/cm<sup>2</sup>). The values of current density were increase as Al was added into SAC105 solder. However, the current density is found to be the lowest for 0.1wt-% Al in comparison to other Al-containing alloys, thus indicating the stability of the formation of passive film on the surface which might be contributes by Al and Sn at this content. Al content 1.0wt-% increases the passivation current density, thereby destabilizing the passive film and resulting in a higher rate of corrosion of the alloy. These results are in accordance with that obtained by Mohanty and Lin (2006a). They reported that solder with the lowest Al content has lowest current density.

Further increase in the potential beyond E shows a sharp increase in current, indicates the transpassive region which might be due to the breakdown of the passive film by incorporation of  $\text{Cl}^-$  anion into the oxide layer, leading to localized corrosion. Previous study (Pistorius & Burstein, 1994) reported that the film was mechanically breakdown due to the penetration of chloride ions into the oxide film and form solid metal chloride.

The overall view from Fig. 4.6 shows the addition of Al shifted the corrosion current density and passivation current density towards more positive values. This suggested that SAC105+1.0Al solder alloy has lowest corrosion resistance. Higher content of Al in the Sn-1.0Ag-0.5Cu-XAl alloy enhances corrosion. These changes are also reflected in the corrosion rate as shown in Table 4.5.

#### **4.3.2 Corrosion rate**

The corrosion rate was obtained by Tafel fit using Gamry Echem Analyst DC105 software and the data was listed in Table 4.5. From Table 4.5, it is seen that SAC105 solder alloy shows the lowest corrosion rate, 0.07 mpy. When 0.1wt-% of Al was added, the corrosion rate was slightly increased to 0.08 mpy. Corrosion rate of SAC105 solder alloy kept increasing to 1.44 mpy and 1.49 mpy when 0.5wt-% and 1.0wt-% Al was added respectively. As a result, it can be concluded that SAC105+1.0Al solder alloy deteriorates and corrodes more rapidly with the low corrosion resistance and highest corrosion rate.

### 4.3.3 Morphological, elemental and phases analyses of corrosion products

The SEM micrograph in Figure 4.7a shows the formation of platelet-like corrosion products on SAC105 solder alloy. However, upon addition of Aluminium, the size of the corrosion products seems to smaller as shown in the Figure 7b-c.

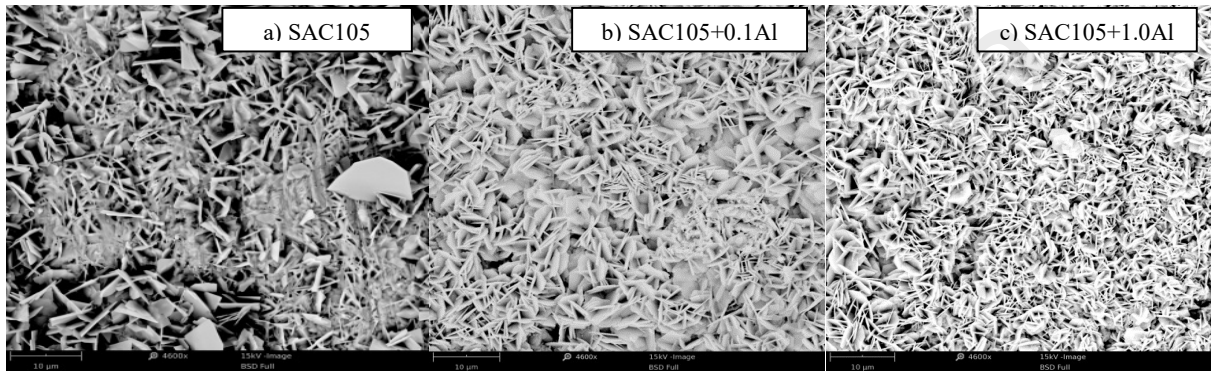


**Figure 4. 7:** SEM micrographs (4600x) of (a) SAC105, (b) SAC105+0.1Al and (c) SAC105+1.0Al solder alloys after polarization test

Table 4.6 shows the surface element concentrations of sample corrosion products as determined by EDS. According to the EDS analysis, the corrosion products on SAC105 solder alloy contained mainly Sn, Cl and O, at 19.3wt-%, 18.5wt-%, and 60.8wt-%, respectively. It is noted that the presence of Cl<sup>-</sup> on the surface and the quantity of this ion increase with Al content. This suggested that Cl may have greater influence on the formation of Al-based corrosion products.

The corrosion products formed on the surface can determine the corrosion resistance of the solder. When corrosion products are more compact, it protects the surface more stable and blocks the access of the active species to the surface and reducing the corrosion rate. Based on the Fig. 4.7, the corrosion products formed on the coupon are found to be smaller in size

and less compact when Al was added into SAC105. Therefore, the corrosion resistance of SAC105 solder alloy is higher than Al-containing solder alloy.

**Table 4. 6:** Mass percentage of elements present in different alloy surfaces after potentiodynamic polarization test.

Mass percentage	Sn	Cl	O	Al
SAC105	19.3	18.5	60.8	-
SAC105+0.1Al	30.5	20.6	47.8	0.4
SAC105+1.0Al	39.3	28.4	31.0	0.8

Samples which were potentiodynamically treated were subsequently subjected to X-ray diffraction (XRD) analysis as shown in Fig. 4.8. The XRD patterns reveal the presence of  $\text{Sn}_3\text{O}(\text{OH})_2\text{Cl}_2$  (ICDD 00-039-0314),  $\text{SnO}$  (ICDD 98-006-019) and  $\text{SnO}_2$  (ICDD 98-000-9178) on the exposed surface of SAC105.  $\text{Al}(\text{OH})_3$  (ICDD 98-000-6162) and  $\text{Al}_2\text{O}_3$  (ICDD 00-010-0173) were detected on Al-containing solder alloys.

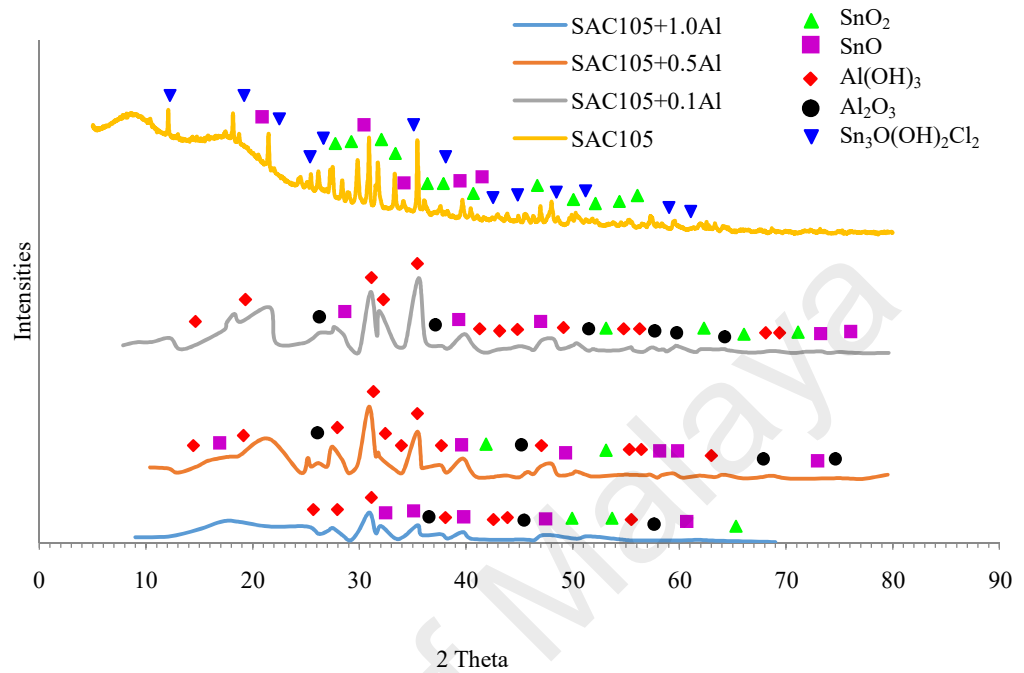
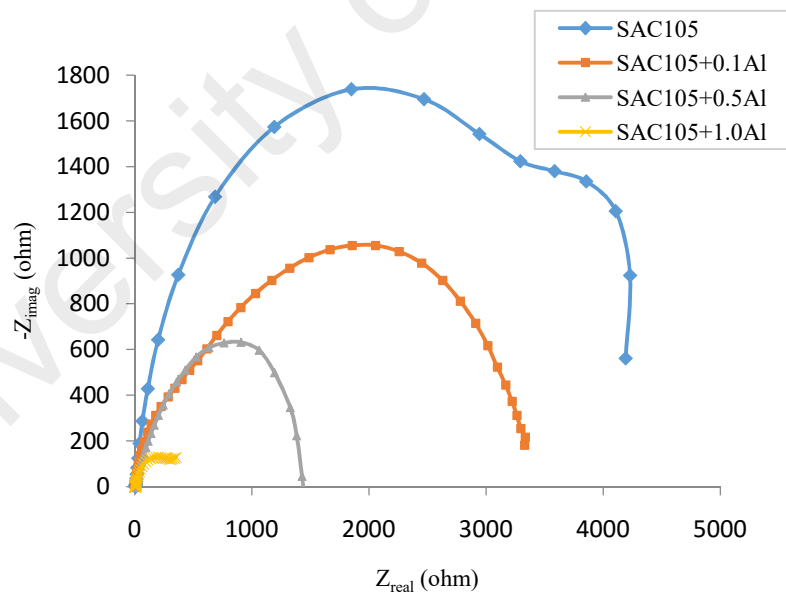


**Figure 4. 8:** X-ray diffraction scans after polarization for SAC105, SAC105+0.1Al, SAC105+0.5Al and SAC105+1.0Al solder alloys in 3.5wt-% NaCl solution

From the XRD analysis in Fig. 4.8, it is seen that  $\text{Sn}_3\text{O}(\text{OH})_2\text{Cl}_2$  was undetectable when Al was added into SAC105 alloy. Instead,  $\text{Al}(\text{OH})_3$  and  $\text{Al}_2\text{O}_3$  appears to be formed on the surface of SAC105+0.1Al, SAC105+0.5Al and SAC105+1.0Al solder alloys. These results were in accordance with the previous study conducted by Mohanty and Lin (2006a) when they studied the effect of Al on the electrochemical corrosion behaviour of Pb free Sn–8.5Zn–0.5Ag–XAl–0.5Ga solder in 3.5wt-% NaCl solution. They reported that there are considerable aluminium segregation occurred towards the surface principally as  $\text{Al}_2\text{O}_3/\text{Al}(\text{OH})_3$  with increase in Al content to 1.5wt-% in the five element solder.

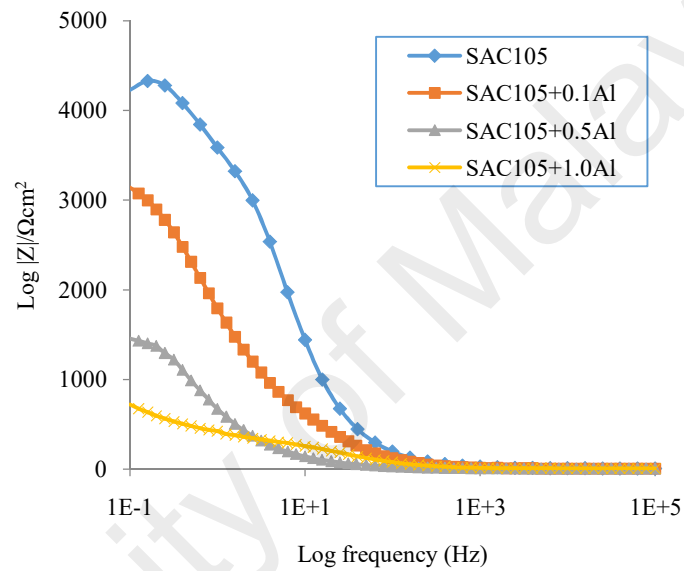
#### 4.3.4 Electrochemical Impedance Spectroscopy (EIS)

Fig. 4.9 displays the Nyquist plots for SAC105, SAC105+0.1Al, SAC105+0.5Al and SAC105+1.0Al solder alloys in 3.5wt-% NaCl solution. As can be seen, the response of the system in the Nyquist complex plane is a semicircle arc for all materials whose diameter decreases with the addition of Al. The diameter of Nyquist semicircle corresponds to the corrosion resistance. It is important to remark that the highest semicircle arc induces the best electrochemical corrosion behaviour. In Fig. 4.9, it is seen that the loop diameter of SAC105 solder alloy is the highest. As the Al was added into SAC105 alloy, the loop diameter was decreased, which indicates the increased corrosion rate and thus the corrosion resistance is reduced with the addition of Al. This observation permits to conclude that the SAC105 solder alloy has the better corrosion resistance as compared to others alloy.



**Figure 4. 9:** Nyquist plot for SAC105, SAC105+0.1Al, SAC105+0.5Al and SAC105+1.0Al solder alloys in 3.5wt-% NaCl solution

Fig. 4.10 presents the impedance spectra, presented as Bode plots for SAC105, SAC105+0.1Al, SAC105+0.5Al and SAC105+1.0Al solder alloys in 3.5wt-% NaCl solution. It is well-known that the corrosion resistance of solder alloys can be determined by  $\log |Z|$  (Fig. 10a) and phase angle  $\theta_{max}$  (Fig. 10b). Higher  $\log |Z|$  and higher  $\theta_{max}$  represent the better corrosion resistance. In the lower frequency region of Bode plots (Fig. 10a), the  $\log |Z|$  tends to decrease with the addition of Al and it has been tabulated in Table 4.7.



**Figure 4.10 a:** Magnitude Bode plot for SAC105, SAC105+0.1Al, SAC105+0.5Al and SAC105+1.0Al solder alloys in 3.5wt-% NaCl solution

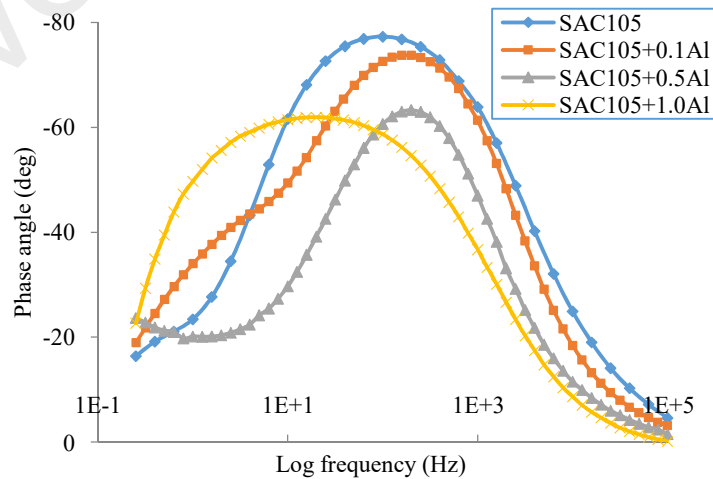


**Figure 4.10 b:** Phase Angle Bode plot for SAC105, SAC105+0.1Al, SAC105+0.5Al and SAC105+1.0Al solder alloys in 3.5wt-% NaCl solution

It can be seen from Fig. 4.10a and Fig. 4.10b that the SAC105 solder alloy exhibits highest magnitude of impedance,  $4229 \Omega \text{ cm}^2$ , and highest  $\theta_{max.}$ ,  $-77.28^\circ$ , indicating the highest corrosion resistance which is attributed to the formation of comparatively more adherent and protective oxide film on the surface. Log  $|Z|$  and  $\theta_{max.}$  tends to decreases with the addition of Al indicates that Al can reduce the corrosion resistance of the solder. From Table 4.7, the value of log  $|Z|$  and  $\theta_{max.}$  decreases to  $3139 \Omega \text{ cm}^2$  and  $-73.72^\circ$  respectively for SAC105+0.1Al and it keep decrease to  $1456 \Omega \text{ cm}^2$  and  $-62.94^\circ$  with the addition of 0.5wt-% Al. At highest concentration of Al (1.0wt-%), SAC105 alloy exhibits lowest log  $|Z|$  ( $719.7 \Omega \text{ cm}^2$ ) and  $\theta_{max.}$  ( $-61.89^\circ$ ). It can be conclude that the addition of Al into SAC105 solder tends to decrease the corrosion resistance of the solder and SAC105 exhibits better corrosion resistance as compared to others.

**Table 4. 7:** Electrochemical impedance spectroscopy parameters for SAC105, SAC105+0.1Al, SAC105+0.5Al and SAC105+1.0Al solder alloys in 3.5wt-% NaCl solution

Solder alloys	Log $ Z (\Omega \text{ cm}^2)$	$\theta_{max.}$ ( $^\circ$ )
SAC105	4229.0	-77.28
SAC105+0.1Al	3139.0	-73.72
SAC105+0.5Al	1456.0	-62.94
SAC105+1.0Al	719.7	-61.89

## CHAPTER 5: CONCLUSIONS AND RECOMMENDATIONS

### 5.1 Conclusions

The following conclusions could be drawn from the present study:

- i. Sn-1.0Ag-0.5Cu solder alloy exhibits better corrosion resistance than Zn-containing solder in 3.5wt-% NaCl solution. It shows higher corrosion potential (-668 mV(SCE)), lower passivation current density (2.56 mA/cm<sup>2</sup>), lower corrosion current density (0.451x10<sup>-3</sup> mA/cm<sup>2</sup>) and a more stable passivation film on the surface.
- ii. The EIS results agreed well with the noble sequence of the four solders with polarization. The sequence of the corrosion resistive solder alloys is: Sn-1.0Ag-0.5Cu > Sn-1.0Ag-0.5Cu-0.1Zn > Sn-1.0Ag-0.5Cu-0.5Zn > Sn-1.0Ag-0.5Cu-1.0Zn. The corrosion resistance of SAC105 is decreased with the increase of Zn concentration.
- iii. XRD analyses shows the presence of SnO, SnO<sub>2</sub>, ZnO and Sn<sub>3</sub>O(OH)<sub>2</sub>Cl<sub>2</sub> compounds on Zn-containing SAC105 solder alloys. The corrosion product, tin oxychloride (Sn<sub>3</sub>O(OH)<sub>2</sub>Cl<sub>2</sub>) is the major and common ones for all solder alloys. This product seems to have a platelet-like structure with a different size and distributed with different orientations.
- iv. Corrosion current density of SAC105 alloy was moderately increased when it is doped with 0.1-0.5% Zn but the current density is drastically increased upon addition of 1% Zn. This finding agrees well with impedance results suggesting that addition of more than 0.5% Zn decreases the corrosion resistance of SAC105 alloy to a higher extent.
- v. The corrosion current densities of SAC105+0.1Al, SAC105+0.5Al and SAC105+1.0Al solder alloy are 0.526 x 10<sup>-3</sup>, 11.1 x 10<sup>-3</sup> and 11.6 x 10<sup>-3</sup> mA/cm<sup>2</sup> respectively. With the increase of Aluminium concentration in SAC105 solder alloy, the corrosion current density and polarization resistance increases and decreases respectively. This corrosion

behavior seems to be attributed to anodic dissolution of Aluminium and followed by Sn- matrix. Therefore, it can be conclude that the addition of Al decrease the corrosion resistance of the SAC105 solder alloy.

- vi. The common corrosion products form on SAC105 include SnO, SnO<sub>2</sub> and Sn<sub>3</sub>O(OH)<sub>2</sub>Cl<sub>2</sub>. It is seen that Sn<sub>3</sub>O(OH)<sub>2</sub>Cl<sub>2</sub> was undetectable when Al was added into SAC105 alloy. Instead, Al(OH)<sub>3</sub> and Al<sub>2</sub>O<sub>3</sub> appears to be formed on SAC105+0.1Al, SAC105+0.5Al and SAC105+1.0Al solder surface.
- vii. Electrochemical Impedance Spectroscopy measurements show that SAC105 solder alloy has the best electrochemical corrosion resistance. As Al was added into SAC105 alloy, the loop diameter was decreased which indicates the increased corrosion rate. Therefore corrosion resistance is reduced with the addition of Al. This observation permits to conclude that the SAC105 solder alloy has the better corrosion resistance as compared to others alloys.

## **5.2 Recommendations for Future Work:**

Sn-3Ag-0.5Cu solder alloy is the best replacement for tin-lead alloy. However, Ag is an expansive metal. Therefore, Sn-1.0Ag-0.5Cu was used in this study. Unfortunately, when the composition of Ag is decreased, the mechanical properties of the solder were not effectively improved. To overcome these issues, alloying element such as Zn, Al etc were added. Previous study by other researchers focused more in improving mechanical properties of these alloys. But there is a lack of information about the corrosion behavior of Sn-Ag-Cu-Zn and Sn-Ag-Cu-Al alloys.

After the corrosion test, we found that the additional of Zn or Al was not improving the corrosion resistance of Sn-1.0Ag-0.5Cu. Hence, further study should be carried out by adding other alloying element in order to improve the corrosion resistance of the solder.

Other recommendations for this study are as below:

- i. Corrosion mechanisms of lead-free solder alloys should be studied in details.
- ii. Corrosion behavior of lead-free solder alloys with different alloying element, composition could be studied more.
- iii. Other experiment such as immersion test should be conducted to double confirm the results obtained through potentiodynamic polarization test and electrochemical impedance spectroscopy (EIS) tests.
- iv. Effect of temperature and exposure duration of lead-free solder alloys in corrosive media should be investigated.

## REFERENCES

- Abosheisha, H., Abdel, N. A., & Fouda, A. (2012). Electrochemical and mechanical behavior of sn-zn-x lead free solders. *Journal of Materials and Environment Science*, 3(3), 452-460.
- Abteu, M., & Selvaduray, G. (2000). Lead-free Solders in Microelectronics. *Materials Science and Engineering: R: Reports*, 27(5), 95-141. doi: [https://doi.org/10.1016/S0927-796X\(00\)00010-3](https://doi.org/10.1016/S0927-796X(00)00010-3)
- Ahmido, A., Sabbar, A., Zouihri, H., Dakhsi, K., Guedira, F., Serghini-Idrissi, M., & El Hajjaji, S. (2011). Effect of bismuth and silver on the corrosion behavior of Sn-9Zn alloy in NaCl 3wt.% solution. *Materials Science and Engineering: B*, 176(13), 1032-1036. doi: <https://doi.org/10.1016/j.mseb.2011.05.034>
- Anderson, I. E., Foley, J. C., Cook, B. A., Haringa, J., Terpstra, R. L., & Unal, O. (2001). Alloying effects in near-eutectic Sn-Ag-Cu solder alloys for improved microstructural stability. *Journal of Electronic Materials*, 30(9), 1050-1059. doi: 10.1007/s11664-001-0129-5
- Anderson, I. E., Walleiser, J., & Haringa, J. L. (2007). Observations of nucleation catalysis effects during solidification of SnAgCuX solder joints. *JOM*, 59(7), 38-43. doi: 10.1007/s11837-007-0087-3
- Andersson, C., & Liu, J. (2008). Effect of corrosion on the low cycle fatigue behavior of Sn-4.0Ag-0.5Cu lead-free solder joints. *International Journal of Fatigue*, 30(5), 917-930. doi: <https://doi.org/10.1016/j.ijfatigue.2007.06.009>
- Assaf, F., El-Rehiem, S. A., & Zaky, A. (1999). Pitting corrosion of zinc in neutral halide solutions. *Materials Chemistry and Physics*, 58(1), 58-63. doi: [https://doi.org/10.1016/S0254-0584\(98\)00253-3](https://doi.org/10.1016/S0254-0584(98)00253-3)
- Bashir, M. N., Haseeb, A. S. M. A., Rahman, A. Z. M. S., Fazal, M. A., & Kao, C. R. (2015). Reduction of electromigration damage in SAC305 solder joints by adding Ni nanoparticles through flux doping. *Journal of Materials Science*, 50(20), 6748-6756. doi: 10.1007/s10853-015-9230-7
- Basics of Electrochemical Impedance Spectroscopy. (n.d.). Retrieved April, 2018, from <https://www.gamry.com/assets/Application-Notes/Basics-of-EIS.pdf>
- Bastecki, C. (1999). A Benchmark Process For the Lead-Free Assembly of Mixed Technology PCB's.

- Bilek, J., Atkinson, J. K., & Wakeham, W. A. (2006). Thermal Conductivity of Molten Lead-Free Solders. *International Journal of Thermophysics*, 27(1), 92-102. doi: 10.1007/s10765-006-0035-4
- Billah, M. M., Shorowordi, K. M., & Sharif, A. (2014). Effect of micron size Ni particle addition in Sn-8Zn-3Bi lead-free solder alloy on the microstructure, thermal and mechanical properties. *Journal of Alloys and Compounds*, 585, 32-39. doi: <https://doi.org/10.1016/j.jallcom.2013.09.131>
- Bobina, M., Kellenberger, A., Millet, J.-P., Muntean, C., & Vaszilcsin, N. (2013). Corrosion resistance of carbon steel in weak acid solutions in the presence of l-histidine as corrosion inhibitor. *Corrosion Science*, 69, 389-395. doi: <https://doi.org/10.1016/j.corsci.2012.12.020>
- Brundle, C. R., Evans, C. A., & Wilson, S. (1992). *Encyclopedia of Materials Characterization: Surfaces, Interfaces, Thin Films*. In C. A. Evans, S. Wilson & C. R. Brundle (Series Eds.),
- Buckley, D. H. (1981). *Surface Effects in Adhesion, Friction, Wear, and Lubrication* Retrieved from [https://books.google.com.my/books?id=EZw\\_rgEACAAJ](https://books.google.com.my/books?id=EZw_rgEACAAJ)
- Chang, T.-C., Hon, M.-H., Wang, M.-C., & Lin, D.-Y. (2004). Electrochemical Behaviors of the Sn-9Zn-xAg Lead-Free Solders in a 3.5 wt % NaCl Solution. *Journal of the Electrochemical Society*, 151(7), C484-C491.
- Chang, T.-C., Wang, J.-W., Wang, M.-C., & Hon, M.-H. (2006). Solderability of Sn-9Zn-0.5Ag-1In lead-free solder on Cu substrate: Part 1. Thermal properties, microstructure, corrosion and oxidation resistance. *Journal of Alloys and Compounds*, 422(1), 239-243. doi: <https://doi.org/10.1016/j.jallcom.2005.09.094>
- Che, F. X., Zhu, W. H., Poh, E. S. W., Zhang, X. W., & Zhang, X. R. (2010). The study of mechanical properties of Sn-Ag-Cu lead-free solders with different Ag contents and Ni doping under different strain rates and temperatures. *Journal of Alloys and Compounds*, 507(1), 215-224. doi: <https://doi.org/10.1016/j.jallcom.2010.07.160>
- Cheng, S.-C., & Lin, K.-L. (2005). Microstructure and Mechanical Properties of Sn-8.55Zn-1Ag-XAl Solder Alloys. *MATERIALS TRANSACTIONS*, 46(1), 42-47. doi: 10.2320/matertrans.46.42
- Choi, J.-W., Cha, H.-S., & Oh, T.-S. (2002). Mechanical Properties and Shear Strength of Sn-3.5Ag-Bi Solder Alloys. *MATERIALS TRANSACTIONS*, 43(8), 1864-1867. doi: 10.2320/matertrans.43.1864

- Chuang, T.-H., Wu, M. W., Chang, S. Y., Ping, S. F., & Tsao, L. C. (2011). Strengthening mechanism of nano-Al<sub>2</sub>O<sub>3</sub> particles reinforced Sn<sub>3.5</sub>Ag<sub>0.5</sub>Cu lead-free solder. *Journal of Materials Science: Materials in Electronics*, 22(8), 1021-1027. doi: 10.1007/s10854-010-0253-1
- Davies, G. (2003). *Materials for Automobile Bodies*. Retrieved from <https://books.google.com.my/books?id=IVTYEHgfrWsC>
- Despić, A. R., Dražić, D. M., Purenović, M. M., & Ciković, N. (1976). Electrochemical properties of aluminium alloys containing indium, gallium and thallium. *Journal of Applied Electrochemistry*, 6(6), 527-542. doi: 10.1007/bf00614541
- Drogowska, M., Ménard, H., & Brossard, L. (1991). Electrochemical behaviour of tin in bicarbonate solution at pH 8. *Journal of Applied Electrochemistry*, 21(1), 84-90. doi: 10.1007/bf01103835
- El-Daly, A. A., & Hammad, A. E. (2010). Effects of small addition of Ag and/or Cu on the microstructure and properties of Sn–9Zn lead-free solders. *Materials Science and Engineering: A*, 527(20), 5212-5219. doi: <https://doi.org/10.1016/j.msea.2010.04.078>
- El-Daly, A. A., Hammad, A. E., Al-Ganainy, G. A., & Ibrahiem, A. A. (2013). Enhancing mechanical response of hypoeutectic Sn–6.5Zn solder alloy using Ni and Sb additions. *Materials & Design (1980-2015)*, 52, 966-973. doi: <https://doi.org/10.1016/j.matdes.2013.06.023>
- El-Daly, A. A., Swilem, Y., Makled, M. H., El-Shaarawy, M. G., & Abdraboh, A. M. (2009). Thermal and mechanical properties of Sn–Zn–Bi lead-free solder alloys. *Journal of Alloys and Compounds*, 484(1), 134-142. doi: <https://doi.org/10.1016/j.jallcom.2009.04.108>
- Ervina, E. M. N., & Amares, S. (2014). Review on the effect of alloying element and nanoparticle additions on the properties of Sn-Ag-Cu solder alloys. *Soldering & Surface Mount Technology*, 26(3), 147-161. doi: doi:10.1108/SSMT-02-2014-0001
- Fayeka, M., Haseeb, A. S. M. A., & Fazal, M. A. (2017). Electrochemical Corrosion Behaviour of Pb-free SAC 105 and SAC 305 Solder Alloys: A Comparative Study. *Sains Malaysiana*, 46(2), 295-302.
- Gabrielli, C., & Group, S. I. (1980). Identification of Electrochemical Processes by Frequency Response Analysis. <https://books.google.com.my/books?id=7DRlygAACAAJ>

- Garcia, L. R., Osório, W. R., Peixoto, L. C., & Garcia, A. (2010). Mechanical properties of Sn–Zn lead-free solder alloys based on the microstructure array. *Materials Characterization*, 61(2), 212-220. doi: <https://doi.org/10.1016/j.matchar.2009.11.012>
- Gebhardt, E., & Petzow, G. (1959). Over structure of silver-copper-tin systems. *Z Metallkde*, 50, 597-605.
- Glaeser, W. A. (2010). *Characterization of Tribological Materials*. In W. A. Glaeser, C. R. Brundle & C. A. Evans (Series Eds.), Retrieved from <https://books.google.com.my/books?id=A0cQ8xPX6esC>
- Glazer, J. (1994). Microstructure and mechanical properties of Pb-free solder alloys for low-cost electronic assembly: A review. *Journal of Electronic Materials*, 23(8), 693-700. doi: 10.1007/bf02651361
- Gouda, E. S., & Aziz, H. A. (2012). Effect of Bi additions on structure and properties of Sn-9Zn-1Ag lead-free solder alloys. *Journal of Materials Science and Engineering: B*, 2(6), 381-388.
- Guo, F., Choi, S., Subramanian, K. N., Bieler, T. R., Lucas, J. P., Achari, A., & Paruchuri, M. (2003). Evaluation of creep behavior of near-eutectic Sn–Ag solders containing small amount of alloy additions. *Materials Science and Engineering: A*, 351(1), 190-199. doi: [https://doi.org/10.1016/S0921-5093\(02\)00853-5](https://doi.org/10.1016/S0921-5093(02)00853-5)
- Guo, F., Lee, J., Choi, S., Lucas, J. P., Bieler, T. R., & Subramanian, K. N. (2001). Processing and aging characteristics of eutectic Sn-3.5Ag solder reinforced with mechanically incorporated Ni particles. *Journal of Electronic Materials*, 30(9), 1073-1082. doi: 10.1007/s11664-001-0132-x
- Hammad, A. E. (2013). Investigation of microstructure and mechanical properties of novel Sn–0.5Ag–0.7Cu solders containing small amount of Ni. *Materials & Design*, 50, 108-116. doi: <https://doi.org/10.1016/j.matdes.2013.03.010>
- Hassam, S., Dichi, E., & Legendre, B. (1998). Experimental equilibrium phase diagram of the Ag–Bi–Sn system. *Journal of Alloys and Compounds*, 268(1), 199-206. doi: [https://doi.org/10.1016/S0925-8388\(97\)00617-8](https://doi.org/10.1016/S0925-8388(97)00617-8)
- Huang, M. L., & Wang, L. (2005). Effects of Cu, Bi, and In on microstructure and tensile properties of Sn-Ag-X(Cu, Bi, In) solders. *Metallurgical and Materials Transactions A*, 36(6), 1439-1446. doi: 10.1007/s11661-005-0236-7

- Huang, M. L., Wang, L., & Wu, C. M. L. (2012). Creep behavior of eutectic Sn–Ag lead-free solder alloy. *Journal of Materials Research*, 17(11), 2897-2903. doi: 10.1557/JMR.2002.0420
- JM Bullion. Silver spot price & charts. Retrieved February 2017, from <http://www.jmbullion.com/charts/silver-prices>
- Kar, A., Ghosh, M., Ray, A. K., & Ghosh, R. N. (2007). Effect of copper addition on the microstructure and mechanical properties of lead free solder alloy. *Materials Science and Engineering: A*, 459(1), 69-74. doi: <https://doi.org/10.1016/j.msea.2006.12.084>
- Kariya, Y., & Otsuka, M. (1998). Mechanical fatigue characteristics of Sn-3.5Ag-X (X=Bi, Cu, Zn and In) solder alloys. *Journal of Electronic Materials*, 27(11), 1229-1235. doi: 10.1007/s11664-998-0074-7
- Kim, K. S., Huh, S. H., & Sukanuma, K. (2003). Effects of intermetallic compounds on properties of Sn–Ag–Cu lead-free soldered joints. *Journal of Alloys and Compounds*, 352(1), 226-236. doi: [https://doi.org/10.1016/S0925-8388\(02\)01166-0](https://doi.org/10.1016/S0925-8388(02)01166-0)
- Kim, K. S., Ryu, K. W., Yu, C. H., & Kim, J. M. (2005). The formation and growth of intermetallic compounds and shear strength at Sn–Zn solder/Au–Ni–Cu interfaces. *Microelectronics Reliability*, 45(3), 647-655. doi: <https://doi.org/10.1016/j.microrel.2004.07.005>
- King, J. A. (1988). *Materials Handbook for Hybrid Microelectronics*. In J. A. King (Series Ed.) Retrieved from <https://books.google.com.my/books?id=SR9TAAAAMAAJ>
- Kinloch, A. J. (1982). *Surface and Interface Analysis* (D. M. Brewis Ed. Vol. 4). London.
- Kostov, A., Milosavljevic, A., Gomidzelovic, L., & Todorovic, R. (2009). *Lead-free alloys for ecological solders manufacturing*. Paper presented at the 9th International Multidisciplinary Scientific GeoConference.
- Kotadia, H. R., Howes, P. D., & Mannan, S. H. (2014). A review: On the development of low melting temperature Pb-free solders. *Microelectronics Reliability*, 54(6), 1253-1273. doi: <https://doi.org/10.1016/j.microrel.2014.02.025>
- Kotadia, H. R., Mokhtari, O., Clode, M. P., Green, M. A., & Mannan, S. H. (2012). Intermetallic compound growth suppression at high temperature in SAC solders

with Zn addition on Cu and Ni-P substrates. *Journal of Alloys and Compounds*, 511(1), 176-188. doi: <https://doi.org/10.1016/j.jallcom.2011.09.024>

Kumar, V., Fang, Z. Z., Liang, J., & Dariavach, N. (2006). Microstructural analysis of lead-free solder alloys. *Metallurgical and Materials Transactions A*, 37(8), 2505-2514. doi: 10.1007/bf02586223

Lecture 11: Electrochemical Techniques. (n.d.). Retrieved April 2018, from [http://www.corrosionclinic.com/corrosion\\_online\\_lectures/ME303L11.HTM](http://www.corrosionclinic.com/corrosion_online_lectures/ME303L11.HTM)

Lee, H., Lin, H., Lee, C., & Chen, P. (2005). Reliability of Sn-Ag-Sb lead-free solder joints. *Materials Science and Engineering: A*, 407(1), 36-44. doi: <https://doi.org/10.1016/j.msea.2005.07.049>

Lee, N.-C., Slattery, J. A., Sovinsky, J. R., Artaki, I., & Vianco, P. T. (1995). *A Drop-In Lead-Free Solder Replacement*. Paper presented at the Proceedings of NEPCON West Conference, Anaheim, CA.

Li, D., Conway, P. P., & Liu, C. (2008). Corrosion characterization of tin-lead and lead free solders in 3.5wt.% NaCl solution. *Corrosion Science*, 50(4), 995-1004. doi: <https://doi.org/10.1016/j.corsci.2007.11.025>

Liang, J., Dariavach, N., & Shangguan, D. (2007). Solidification Condition Effects on Microstructures and Creep Resistance of Sn-3.8Ag-0.7Cu Lead-Free Solder. *Metallurgical and Materials Transactions A*, 38(7), 1530-1538. doi: 10.1007/s11661-007-9222-6

Lin, H.-J., & Chuang, T.-H. (2010). Effects of Ce and Zn additions on the microstructure and mechanical properties of Sn-3Ag-0.5Cu solder joints. *Journal of Alloys and Compounds*, 500(2), 167-174. doi: <https://doi.org/10.1016/j.jallcom.2010.03.233>

Lin, K.-L., Chung, F.-C., & Liu, T.-P. (1998). The potentiodynamic polarization behavior of Pb-free XIn-9(5Al-Zn)-YSn solders. *Materials Chemistry and Physics*, 53(1), 55-59. doi: [https://doi.org/10.1016/S0254-0584\(97\)02062-2](https://doi.org/10.1016/S0254-0584(97)02062-2)

Lin, K.-L., & Liu, T.-P. (1998a). The electrochemical corrosion behaviour of Pb-free Al-Zn-Sn solders in NaCl solution. *Materials Chemistry and Physics*, 56(2), 171-176. doi: [https://doi.org/10.1016/S0254-0584\(98\)00171-0](https://doi.org/10.1016/S0254-0584(98)00171-0)

Lin, K.-L., & Liu, T.-P. (1998b). High-Temperature Oxidation of a Sn-Zn-Al Solder. *Oxidation of Metals*, 50(3), 255-267. doi: 10.1023/a:1018840405283

- Lin, K.-L., & Wen, L.-H. (1998). The wetting of copper by Al–Zn–Sn solders. *Journal of Materials Science: Materials in Electronics*, 9(1), 5-8. doi: 10.1023/a:1008970615193
- Liu, C.-Y., Chen, Y.-R., Li, W.-L., Hon, M.-H., & Wang, M.-C. (2007). Electrochemical Properties of Joints Formed Between Sn-9Zn-1.5Ag-1Bi Alloys and Cu Substrates in a 3.5 wt.% NaCl Solution. *Journal of Electronic Materials*, 36(11), 1531-1535. doi: 10.1007/s11664-007-0221-6
- Luo, W. C., Ho, C. E., Tsai, J. Y., Lin, Y. L., & Kao, C. R. (2005). Corrosion behavior of Zn-containing solder alloys in 3.5wt-% NaCl solution. *Materials Science and Engineering: A*, 396, 385-391.
- Madeni, J. C., Liu, S. X., & Siewert, T. A. (2003). *Intermetallics formation and growth at the interface of tin-based solder alloys and copper substrates*. Paper presented at the Brazing and Soldering Conference.
- Massalski, T. B., Okamoto, H., Subramanian, P. R., & Kacprzak, L. (1990). Binary Alloy Phase Diagrams. (v. 2). [https://books.google.com.my/books?id=xG\\_1QgAACAAJ](https://books.google.com.my/books?id=xG_1QgAACAAJ)
- McCormack, M., & Jin, S. (1993). Progress in the design of new lead-free solder alloys. *JOM*, 45(7), 36-40. doi: 10.1007/bf03222379
- McCormack, M., & Jin, S. (1994). New, lead-free solders. *Journal of Electronic Materials*, 23(7), 635-640. doi: 10.1007/bf02653349
- Miller, W. S., Zhuang, L., Bottema, J., Wittebrood, A. J., De Smet, P., Haszler, A., & Vieregge, A. (2000). Recent development in aluminium alloys for the automotive industry. *Materials Science and Engineering: A*, 280(1), 37-49. doi: [https://doi.org/10.1016/S0921-5093\(99\)00653-X](https://doi.org/10.1016/S0921-5093(99)00653-X)
- Miyoshi, K., & Chung, Y. (1993). *Surface Diagnostics in Tribology: Fundamental Principles and Applications*. Retrieved from <https://books.google.com.my/books?id=cgVw6rYiD9EC>
- Mohanty, U. S., & Lin, K.-L. (2006a). Effect of Al on the electrochemical corrosion behaviour of Pb free Sn–8.5 Zn–0.5 Ag–XAl–0.5 Ga solder in 3.5% NaCl solution. *Applied Surface Science*, 252(16), 5907-5916. doi: <https://doi.org/10.1016/j.apsusc.2005.08.020>

- Mohanty, U. S., & Lin, K.-L. (2006b). The effect of alloying element gallium on the polarization characteristics of Pb-free Sn–Zn–Ag–Al–XGa solders in NaCl solution. *Corrosion Science*, 48(3), 662-678. doi: <https://doi.org/10.1016/j.corsci.2005.02.003>
- Mohanty, U. S., & Lin, K.-L. (2006c). Potentiodynamic Polarization Measurement of Sn–8.5Zn–XAl–0.5Ga Alloy in 3.5% NaCl Solution. *Journal of the Electrochemical Society*, 153(8), B319-B324. doi: 10.1149/1.2209569
- Moon, K.-W., Boettinger, W. J., Kattner, U. R., Biancaniello, F. S., & Handwerker, C. A. (2000). Experimental and thermodynamic assessment of Sn–Ag–Cu solder alloys. *Journal of Electronic Materials*, 29(10), 1122-1136. doi: 10.1007/s11664-000-0003-x
- Nazeri, M. F. M., & Mohamad, A. A. (2014). Corrosion measurement of Sn–Zn lead-free solders in 6M KOH solution. *Measurement*, 47, 820-826. doi: <https://doi.org/10.1016/j.measurement.2013.10.002>
- Noh, B.-I., Choi, J.-H., Yoon, J.-W., & Jung, S.-B. (2010). Effects of cerium content on wettability, microstructure and mechanical properties of Sn–Ag–Ce solder alloys. *Journal of Alloys and Compounds*, 499(2), 154-159. doi: <https://doi.org/10.1016/j.jallcom.2010.03.179>
- Oberg, E., & Jones, F. D. (1988). *Machinery's Handbook, 23rd Revised Edition*
- Osório, W. R., Freitas, E. S., Spinelli, J. E., & Garcia, A. (2014). Electrochemical behavior of a lead-free Sn–Cu solder alloy in NaCl solution. *Corrosion Science*, 80, 71-81. doi: <https://doi.org/10.1016/j.corsci.2013.11.010>
- Osório, W. R., Garcia, L. R., Peixoto, L. C., & Garcia, A. (2011). Electrochemical behavior of a lead-free SnAg solder alloy affected by the microstructure array. *Materials & Design*, 32(10), 4763-4772. doi: <https://doi.org/10.1016/j.matdes.2011.06.032>
- Osório, W. R., Spinelli, J. E., Afonso, C. R. M., Peixoto, L. C., & Garcia, A. (2011). Microstructure, corrosion behaviour and microhardness of a directionally solidified Sn–Cu solder alloy. *Electrochimica Acta*, 56(24), 8891-8899. doi: <https://doi.org/10.1016/j.electacta.2011.07.114>
- Paul, V. B. (2010). Solder Alloys: Physical and Mechanical Properties. Retrieved 26 Nov. 2015, from [http://alafir.com/reference/solder\\_alloys/](http://alafir.com/reference/solder_alloys/)

- Pistorius, P. C., & Burstein, G. T. (1994). Aspects of the effects of electrolyte composition on the occurrence of metastable pitting on stainless steel. *Corrosion Science*, 36(3), 525-538. doi: [https://doi.org/10.1016/0010-938X\(94\)90041-8](https://doi.org/10.1016/0010-938X(94)90041-8)
- Puttlitz, K. J., & Stalter, K. A. (2004). *Handbook of Lead-Free Solder Technology for Microelectronic Assemblies*. Retrieved from <https://books.google.com.my/books?id=H75TywRXUK4C>
- Quinn, T. F. J. (1991). *Physical Analysis for Tribology*. Retrieved from <https://books.google.com.my/books?id=91ZiQgAACAAJ>
- Rana, R. S., Purohit, R., & Das, S. (2012). Reviews on the influences of alloying elements on the microstructure and mechanical properties of aluminum alloys and aluminum alloy composites. *International Journal of Scientific and Research Publications*, 2(6), 1-7.
- Richard, C., & Michael, P. (2004). Questions concerning the migration to lead-free solder. *Circuit World*, 30(2), 34-40. doi: [doi:10.1108/03056120410512226](https://doi.org/10.1108/03056120410512226)
- Richards, B. P. (1999). An analysis of the current status of lead-free soldering.
- Rosalbino, F., Angelini, E., Zanicchi, G., Carlini, R., & Marazza, R. (2009). Electrochemical corrosion study of Sn-3Ag-3Cu solder alloy in NaCl solution. *Electrochimica Acta*, 54(28), 7231-7235. doi: <https://doi.org/10.1016/j.electacta.2009.07.030>
- Rosalbino, F., Angelini, E., Zanicchi, G., & Marazza, R. (2008). Corrosion behaviour assessment of lead-free Sn-Ag-M (M=In, Bi, Cu) solder alloys. *Materials Chemistry and Physics*, 109(2), 386-391. doi: <https://doi.org/10.1016/j.matchemphys.2007.12.006>
- Rotometals. Non-ferrous metals and custom alloys. Retrieved Feb. 2017, from <https://rotometals.com/solder>
- Sabri, M. F. M., Shnawah, D. A., Badruddin, I. A., Said, S. B. M., Che, F. X., & Ariga, T. (2013). Microstructural stability of Sn-1Ag-0.5Cu-xAl (x=1, 1.5, and 2wt.%) solder alloys and the effects of high-temperature aging on their mechanical properties. *Materials Characterization*, 78, 129-143. doi: <https://doi.org/10.1016/j.matchar.2013.01.015>

- Salimin, M. J. (2008). *Properties of low temperature Indium-based ternary lead free solders system*. (Master of Science), Universiti Sains Malaysia. Retrieved from <https://core.ac.uk/download/pdf/11959567.pdf>
- Schaefer, R. J., & Lewis, D. J. (2005). Directional solidification in a AgCuSn eutectic alloy. *Metallurgical and Materials Transactions A*, 36(10), 2775-2783. doi: 10.1007/s11661-005-0273-2
- See, C. W., Yahaya, M. Z., Haliman, H., & Mohamad, A. A. (2016). Corrosion Behavior of Corroded Sn–3.0Ag–0.5Cu Solder Alloy. *Procedia Chemistry*, 19, 847-854. doi: <https://doi.org/10.1016/j.proche.2016.03.112>
- Shen, J., Liu, Y., Wang, D., & Gao, H. (2006). Nano ZrO<sub>2</sub> particulate-reinforced lead-free solder composite. *Journal of Materials Science and Technology -Shenyang-*, 22(4), 529-532.
- Shih, P.-C., & Lin, K.-L. (2011). Interfacial Bonding Behavior with Introduction of Sn–Zn–Bi Paste to Sn–Ag–Cu Ball Grid Array Package During Multiple Reflows. *Journal of Materials Research*, 20(1), 219-229. doi: 10.1557/JMR.2005.0023
- Shohji, I., Gagg, C., & Plumbridge, W. J. (2004). Creep properties of Sn-8Mass%Zn-3Mass%Bi lead-free alloy. *Journal of Electronic Materials*, 33(8), 923-927. doi: 10.1007/s11664-004-0222-7
- Smith, D. R., Siewert, T. A., Stephen, L., & C., M. J. (2002). Database for Solder Properties with Emphasis on New Lead-free Solders. <https://www.nist.gov/None>
- Song, J.-M., & Wu, Z.-M. (2006). Variable eutectic temperature caused by inhomogeneous solute distribution in Sn–Zn system. *Scripta Materialia*, 54(8), 1479-1483. doi: <https://doi.org/10.1016/j.scriptamat.2005.12.056>
- Stirrup, B. N., & Hampson, N. A. (1977). Electrochemical reactions of tin in aqueous electrolytic solutions. *Surface Technology*, 5(6), 429-462. doi: [https://doi.org/10.1016/0376-4583\(77\)90011-5](https://doi.org/10.1016/0376-4583(77)90011-5)
- Subramanian, K. (2007). *Lead-Free Electronic Solders: A Special Issue of the Journal of Materials Science: Materials in Electronics* Retrieved from <https://books.google.com.my/books?id=MDMMd9EaVjcC>

- Suganuma, K. (2001). Advances in lead-free electronics soldering. *Current Opinion in Solid State and Materials Science*, 5(1), 55-64. doi: [https://doi.org/10.1016/S1359-0286\(00\)00036-X](https://doi.org/10.1016/S1359-0286(00)00036-X)
- Suganuma, K., Niihara, K., Shoutoku, T., & Nakamura, Y. (2011). Wetting and interface microstructure between Sn–Zn binary alloys and Cu. *Journal of Materials Research*, 13(10), 2859-2865. doi: 10.1557/JMR.1998.0391
- Swenson, D. (2007). The effects of suppressed beta tin nucleation on the microstructural evolution of lead-free solder joints *Lead-Free Electronic Solders: A Special Issue of the Journal of Materials Science: Materials in Electronics* (pp. 39-54). Boston, MA: Springer US.
- Takemoto, T., Funaki, T., & Matsunawa, A. (1999). Electrochemical Investigation on the Effect of Silver Addition on Wettability of Sn-Zn System Lead-free Solder. *QUARTERLY JOURNAL OF THE JAPAN WELDING SOCIETY*, 17(2), 251-258. doi: 10.2207/qjws.17.251
- Tsao, L. C., & Chang, S. Y. (2010). Effects of Nano-TiO<sub>2</sub> additions on thermal analysis, microstructure and tensile properties of Sn<sub>3.5</sub>Ag<sub>0.25</sub>Cu solder. *Materials & Design*, 31(2), 990-993. doi: 10.1016/j.matdes.2009.08.008
- Tsao, L. C., Chang, S. Y., Lee, C. I., Sun, W. H., & Huang, C. H. (2010). Effects of nano-Al<sub>2</sub>O<sub>3</sub> additions on microstructure development and hardness of Sn<sub>3.5</sub>Ag<sub>0.5</sub>Cu solder. *Materials & Design*, 31(10), 4831-4835. doi: 10.1016/j.matdes.2010.04.033
- Tu, K. N. (2007). *Solder Joint Technology: Materials, Properties, and Reliability* Retrieved from [https://books.google.com.my/books?id=7Zo8qF1a\\_YEC](https://books.google.com.my/books?id=7Zo8qF1a_YEC)
- Walker, I. R. (2011). *Reliability in Scientific Research: Improving the Dependability of Measurements, Calculations, Equipment, and Software* Retrieved from [https://books.google.com.my/books?id=zhX\\_5hccFWMC](https://books.google.com.my/books?id=zhX_5hccFWMC)
- Wu, B. Y., Chan, Y. C., Alam, M. O., & Jillek, W. (2006). Electrochemical corrosion study of Pb-free solders. *Journal of Materials Research*, 21(1), 62-70. doi: 10.1557/jmr.2006.0035
- Wu, C. M. L., Yu, D. Q., Law, C. M. T., & Wang, L. (2002). Microstructure and mechanical properties of new lead-free Sn-Cu-RE solder alloys. *Journal of Electronic Materials*, 31(9), 928-932. doi: 10.1007/s11664-002-0185-5

- Wu, C. M. L., Yu, D. Q., Law, C. M. T., & Wang, L. (2004). Properties of lead-free solder alloys with rare earth element additions. *Materials Science and Engineering: R: Reports*, 44(1), 1-44. doi: <https://doi.org/10.1016/j.mser.2004.01.001>
- Wu, C. M. L., Yu, D. Q., Law, C. M. T., & Wang, L. (2011). Improvements of microstructure, wettability, tensile and creep strength of eutectic Sn–Ag alloy by doping with rare-earth elements. *Journal of Materials Research*, 17(12), 3146-3154. doi: 10.1557/JMR.2002.0455
- Xu, G., Guo, F., Wang, X., Xia, Z., Lei, Y., Shi, Y., & Li, X. (2011). Retarding the electromigration effects to the eutectic SnBi solder joints by micro-sized Ni-particles reinforcement approach. *Journal of Alloys and Compounds*, 509(3), 878-884. doi: <https://doi.org/10.1016/j.jallcom.2010.09.123>
- Xu, J., Liu, X., Li, X., Barbero, E., & Dong, C. (2006). Effect of Sn concentration on the corrosion resistance of Pb-Sn alloys in H<sub>2</sub>SO<sub>4</sub> solution. *Journal of Power Sources*, 155(2), 420-427. doi: <https://doi.org/10.1016/j.jpowsour.2005.04.026>
- Yamamoto, T., & Tsubone, K.-i. (2007). Assembly technology using lead-free solder. *FUJITSU Science Technology*, 43(1), 50-58.
- Yang, L., Zhang, Y., Du, C., Dai, J., & Zhang, N. (2015). Effect of aluminum concentration on the microstructure and mechanical properties of Sn–Cu–Al solder alloy. *Microelectronics Reliability*, 55(3), 596-601. doi: <https://doi.org/10.1016/j.microrel.2014.12.017>
- Yao, P., Liu, P., & Liu, J. (2008). Effects of multiple reflows on intermetallic morphology and shear strength of SnAgCu–xNi composite solder joints on electrolytic Ni/Au metallized substrate. *Journal of Alloys and Compounds*, 462(1), 73-79. doi: <https://doi.org/10.1016/j.jallcom.2007.08.041>
- Yu, S.-P., Liao, C.-L., Hon, M.-H., & Wang, M.-C. (2000). The effects of flux on the wetting characteristics of near-eutectic Sn-Zn-In solder on Cu substrate. *Journal of Materials Science*, 35(17), 4217-4224. doi: 10.1023/a:1004867329163
- Zeng, K., & Tu, K. N. (2002). Six cases of reliability study of Pb-free solder joints in electronic packaging technology. *Materials Science and Engineering: R: Reports*, 38(2), 55-105. doi: [https://doi.org/10.1016/S0927-796X\(02\)00007-4](https://doi.org/10.1016/S0927-796X(02)00007-4)
- Zhang, L., Xue, S. B., Zeng, G., Gao, L. L., & Ye, H. (2012). Interface reaction between SnAgCu/SnAgCuCe solders and Cu substrate subjected to thermal cycling and

isothermal aging. *Journal of Alloys and Compounds*, 510(1), 38-45. doi:  
<https://doi.org/10.1016/j.jallcom.2011.08.044>

Zhou, J., Sun, Y., & Xue, F. (2005). Properties of low melting point Sn–Zn–Bi solders. *Journal of Alloys and Compounds*, 397(1), 260-264. doi:  
<https://doi.org/10.1016/j.jallcom.2004.12.052>

University of Malaya

## LIST OF PUBLICATIONS AND PAPERS PRESENTED

1. N. K. Liyana, M. A. Fazal, A. S. M. A. Haseeb, “Effect of Zn concentration on the corrosion behaviour of SAC105 solder alloy in 3.5wt-% NaCl solution”, International Conference on Science, Technology and Management (ICSTM) 2015 on 9<sup>th</sup> – 10<sup>th</sup> October 2015 at Kuala Lumpur.
2. N. K. Liyana, A. S. M. A. Haseeb, M. A. Fazal, (2017). Polarization and EIS studies to evaluate the effect of Aluminum concentration on the corrosion behavior of SAC105 solder alloy, *Materials Science-Poland*.

University of Malaya